Robotica (2015) volume 33, pp. 768–786. © Cambridge University Press 2014
doi:10.1017/S0263574714000459

Distributed control strategy for flexible link manipulators

Raouf Fareh†*, Mohamad Saad‡ and Maarouf Saad†

†*Electrical Engineering Department, Université du Québec, École de Technologie Supérieure, 1100, rue Notre-Dame ouest, Montréal (Québec), H3C 1K3 Canada*
‡*School of Engineering, Université du Québec en Abitibi-Témiscamingue, 445, boul. de l'Université, Rouyn-Noranda (Québec), J9X 5E4 Canada*

(Accepted February 6, 2014. First published online: March 13, 2014)

SUMMARY
This paper presents a nonlinear distributed control strategy for flexible-link manipulators to solve the tracking control problem in the joint space and cancel vibrations of the links. First, the dynamic of an n-flexible-link manipulator is decomposed into n subsystems. Each subsystem has a pair of one joint and one link. The distributed control strategy is applied to each subsystem starting from the last subsystem. The strategy of control consists in controlling the nth joint and stabilizing the nth link by assuming that the remaining subsystems are stable. Then, going backward to the $(n-1)$th subsystem, the same control strategy is applied to each corresponding joint-link subsystem until the first. Sliding mode technique is used to develop the control law of each subsystem and the global stability of the resulting tracking errors is proved using the Lyapunov technique. This algorithm was tested on a two-flexible-link manipulator and gave effective results, a good tracking performance, and capability to eliminate the links' vibrations.

KEYWORD: Distributed control; Flexible-link manipulators; Sliding mode; Stability; Tracking trajectories.

1. Introduction

There are many advantages of using manipulators with thin and lightweight links in contrast to traditional rigid manipulators. Indeed, flexible-link manipulators have faster response time, lower energy consumption, lower overall mass, low-rated actuators, and, in general, lower overall cost. Due to links' flexibility, the dynamical model of flexible-link manipulators is much more complicated than that of rigid manipulators. As a result of this complicated dynamic model, several challenges in the design and implementation of controllers were motivated. Indeed, the number of controlled variables for a flexible-link manipulator is strictly less than the number of mechanical degrees of freedom (DOF), i.e. it represents an underactuated system. In this case, the control problem is twofold: in addition to motion objectives as in a rigid manipulator, it must also stabilize the vibrations that are naturally excited. Two possible configurations can describe the dynamical model of flexible manipulators. First, the dynamical model can be regarded as one multi-input and multi-output (MIMO) system; one controller is used in this case for all joints and links. Second, the dynamical model can be viewed as interconnected subsystems. Each subsystem has a pair of one joint and one link and is controlled with one controller.

Many control strategies are based on the MIMO representation of the dynamical model of flexible manipulators. In the linear case, a Linear-Quadratic-Gaussian (LQG) approach and the stable factorization technique were used.[1,2] A comparative study of a State-Feedback controller and a Linear Quadratic Regulator (LQR) using the tip deflection feedback measured by a strain gauge were proposed to minimize the link vibrations of a single-link flexible manipulator.[3] A feed forward control was used in ref. [4, 5] to control flexible link manipulators. The feed forward controller design

* Corresponding author. E-mail: raouf.fareh.1@ens.etsmtl.ca

https://doi.org/10.1017/S0263574714000459 Published online by Cambridge University Press

used in ref. [4] is for tracking trajectory of the tip position without any oscillations for one flexible link manipulator. The generalization of the computed-torque method is used for the tracking control of nonlinear flexible-link manipulators.[6,7] The objectives were to track desired trajectories in the joint space and vibration suppression in the links. Adaptive control is used when the system parameters are considered unknown.[8,9] The reinforcement learning (RL) technique is used for developing a real-time adaptive control of a two-link flexible manipulator.[8] The controller consists of a proportional derivative (PD) tracking loop and an adaptive bloc based on RL loop used for tip trajectory control and cancelling the deflection of a two-link flexible manipulator. Intelligent control strategies were also applied to flexible link manipulators.[10–12] Several works used sliding mode to control the flexible link manipulators.[13,14] Sliding mode technique based on a partial feedback linearization controller was used in ref. [14] to achieve set point precision positioning control for a single flexible link manipulator with payload. For a two-flexible-link manipulator, a high-order nonsingular terminal sliding mode optimal control scheme is used to solve the non-minimum phase and chattering problems.[13]

All the previous control schemes use one controller for all joints and links. Unfortunately, when using the dynamical model as one MIMO system, the real-time implementation of these controllers is not easy due to the complexity of their structures.[15] To overcome this problem, the dynamical model of flexible manipulators can be considered as interconnected subsystems. Each subsystem consists of one joint and the corresponding flexible link. Several control schemes used this configuration. Decentralized control is used for flexible links manipulators.[16,17] In ref. [16], the authors used the decentralized control strategy featuring a PD controller for the joint, and an LQR for the link to control two-flexible-link manipulators. A decentralized control strategy composed of a PD controller for the joint, and a linear velocity feedback controller for the flexible link was proposed in ref. [17]. Independent joint control is used for the endpoint position control problem of a two-flexible-link mechanism with very flexible links.[18] The drawback of this method is that the authors used acceleration sensing for acceleration measurement, which is not always available. Using the nonlinear model of flexible manipulators, a hierarchical control strategy to track desired trajectories in the workspace of a two-flexible-link manipulator was developed.[19] A feedback linearization approach is used for each subsystem (a pair of joint and link) to develop control laws. To simplify the real-time implementation we present in this paper, a distributed control strategy is proposed for multi-link flexible manipulators to track desired trajectories in the joint space and to remove link vibration. The control strategy consists to rewrite, at the first time, the dynamical model of n-flexible-links manipulator as n subsystems. Each subsystem contains a pair of one joint and one link. Second, the control strategy consists in starting by controlling the last subsystem while considering the remaining subsystems stable. Then, going backward to the $(n-1)$-th subsystem, the same strategy is applied, and so on, until the first subsystem. The control laws are developed using the sliding mode technique. Lyapunov theory is used to prove the global stability of the error dynamics. This control strategy is implemented on a two-flexible-link manipulator.

This paper is organized as follows: Section 2 presents the description and the modeling of the n-flexible-link manipulator. The distributed control strategy of multi-flexible link and stability analysis of the error dynamics are presented in Section 3. Section 4 presents the experimental results of the proposed control strategy of a two-flexible-link manipulator. Finally, conclusions are given in Section 5.

2. Modeling and Problem Formulation

The n-flexible-link manipulator is shown in Fig. 1. The links are presented in a cascade form and actuated by individual motors. An inertial payload is attached to the end effectors. The motion of each link is assumed to be in the horizontal plane and has a very small deflection. Using Lagrange equations, the dynamical model of an n-DOF flexible manipulator is given by:[20]

$$M(\boldsymbol{q})\ddot{\boldsymbol{q}} + C(\boldsymbol{q}, \dot{\boldsymbol{q}})\dot{\boldsymbol{q}} + D\dot{\boldsymbol{q}} + K\dot{\boldsymbol{q}} = L\boldsymbol{\tau}, \tag{1}$$

where M is the inertia and mass matrix, $C(\boldsymbol{q}, \dot{\boldsymbol{q}})\dot{\boldsymbol{q}}$ is the Coriolis and centrifugal forces vector, D is the friction matrix, and K is the rigidity matrix. Also, $\mathbf{q}$ represents the vector of the generalized coordinates and $\boldsymbol{\tau}$ is the vector of the applied torques.

https://doi.org/10.1017/S0263574714000459 Published online by Cambridge University Press

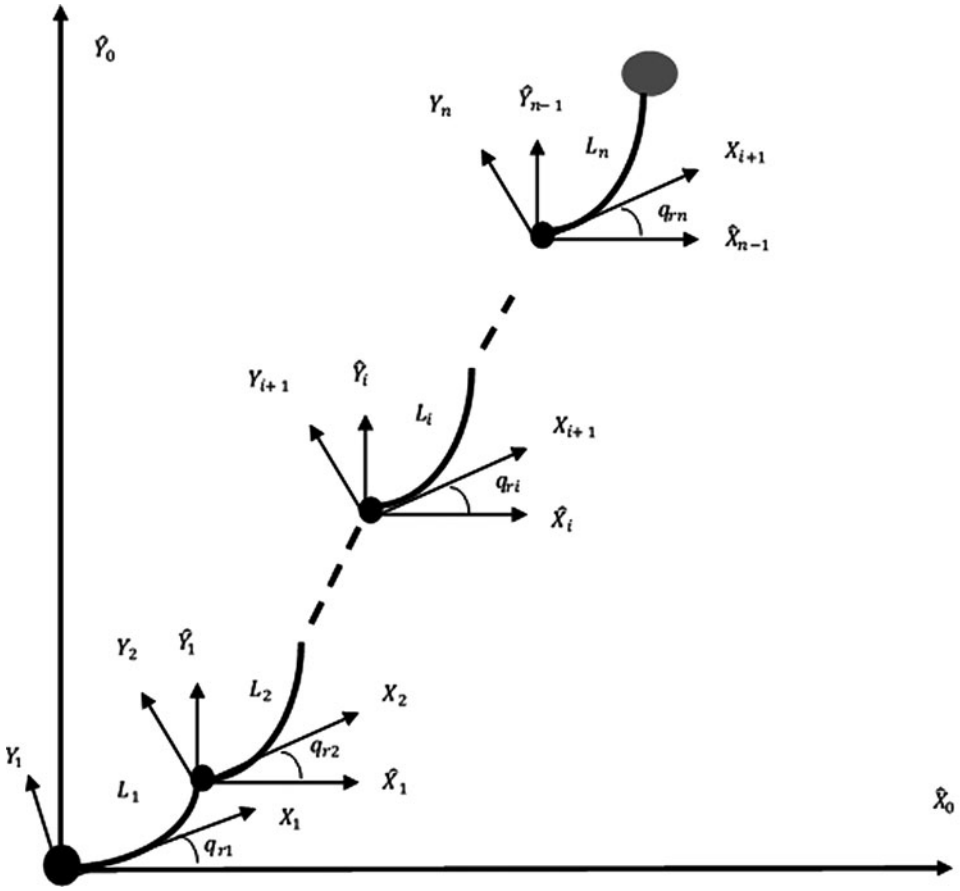


Fig. 1. Flexible-link manipulator.

Note: in the rest of paper, the scalar is written in lower case, the vector in **lower case bold** and the matrix is in upper case.

For the n rigid coordinates and n flexible links, the deformation of the ith flexible link is given by the following equation:

$$v_i(x,t) = \sum_{j=1}^{z_i} \emptyset_{ij}(x) q_{fij}(t) \quad i = 1, \ldots, n, \tag{2}$$

where q_{fij} is the jth generalized flexible coordinate, $\emptyset_{ij}(x)$ is its jth shape function, and z_i is the number of retained flexible modes of the ith flexible link. Note that the total number of flexible modes is $z = \sum_{i=1}^{n} z_i$ and the number of rigid modes is n.

The dynamical model (1) can be written as follows:

$$\begin{bmatrix} [M_r]_{n\times n} & [M_{rf}]_{n\times z} \\ [M_{rf}^T]_{z\times n} & [M_f]_{z\times z} \end{bmatrix}_{(n+z)\times(n+z)} \begin{bmatrix} \ddot{\boldsymbol{q}}_r \\ \ddot{\boldsymbol{q}}_f \end{bmatrix} + \begin{bmatrix} [C_r]_{n\times n} & [C_{rf}]_{n\times z} \\ [C_{rf}^T]_{z\times n} & [C_f]_{z\times z} \end{bmatrix} \begin{bmatrix} \dot{\boldsymbol{q}}_r \\ \dot{\boldsymbol{q}}_f \end{bmatrix}$$
$$+ \begin{bmatrix} 0 & 0 \\ 0 & [D_f]_{z\times z} \end{bmatrix} \begin{bmatrix} \dot{\boldsymbol{q}}_r \\ \dot{\boldsymbol{q}}_f \end{bmatrix} + \begin{bmatrix} 0_{n\times n} & 0_{n\times z} \\ 0_{z\times n} & [K_f]_{z\times z} \end{bmatrix} \begin{bmatrix} \boldsymbol{q}_r \\ \boldsymbol{q}_f \end{bmatrix} = \begin{bmatrix} I_{n\times n} \\ 0_{z\times n} \end{bmatrix} \tau_{n\times 1}, \tag{3}$$

where M_r and M_f are the mass and inertia matrices for the rigid and the flexible parts, respectively. M_{rf} is a coupled element. The subscripts r and f denote the rigid and flexible modes. In this work, we consider only the first flexible mode of each link, then $z = n$.

There exists a non-singular matrix of transformation T_r such as:

$$\bar{\boldsymbol{q}} = T_r \boldsymbol{q}, \tag{4}$$

https://doi.org/10.1017/S0263574714000459 Published online by Cambridge University Press

where $\boldsymbol{q} = [\boldsymbol{q_r}\ \ \boldsymbol{q_f}]^{\mathrm{T}} = [q_{r1}\ \cdots\ q_{rn}\ q_{f1}\ \cdots\ q_{fn}]^{\mathrm{T}}$ is the original generalized coordinate, $\bar{\boldsymbol{q}} = [\boldsymbol{q}_1\ \cdots\ \boldsymbol{q}_i\ \cdots\ \boldsymbol{q_n}]^{\mathrm{T}} = [q_{r1}\ \ q_{f1}\ \cdots\ q_{ri}\ \ q_{fi}\ \ \ldots\ q_{rn}\ \ q_{fn}]^{\mathrm{T}}$ is the transformed one, $\boldsymbol{q_i} = [q_{ri}\ \ q_{fi}]^{\mathrm{T}}$ is the generalized coordinate associated with the ith subsystem (ith joint and link) and the matrix of transformation T_r is given by:

$$T_r = \begin{array}{c} \\ 1 \\ \\ \\ \\ \\ \\ \\ \\ 2n \end{array} \begin{bmatrix} \overbrace{1\ 2 \quad\quad i \quad\quad n}^{} & \overbrace{n{+}1 \quad\quad n{+}i \quad\quad 2n}^{} \\ 1\,0\ldots0\,0\,0\ldots0\,0\,0 & 0\,0\ldots0\,0\,0\ldots0\,0\,0 \\ 0\,0\ldots0\,0\,0\ldots0\,0\,0 & 1\,0\ldots0\,0\,0\ldots0\,0\,0 \\ & \vdots \\ & \vdots \\ 0\,0\ldots0\,1\,0\ldots0\,0\,0 & 0\,0\ldots0\,0\,0\ldots0\,0\,0 \\ 0\,0\ldots0\,0\,0\ldots0\,0\,0 & 0\,0\ldots0\,1\,0\ldots0\,0\,0 \\ & \vdots \\ & \vdots \\ 0\,0\ldots0\,0\,0\ldots0\,0\,1 & 0\,0\ldots0\,0\,0\ldots0\,0\,0 \\ 0\,0\ldots0\,0\,0\ldots0\,0\,0 & 0\,0\ldots0\,0\,0\ldots0\,0\,1 \end{bmatrix}. \tag{5}$$

Using the previous transformation, the dynamical model (1) can be written as follows:

$$M(\boldsymbol{q})\,T_r^{-1}\ddot{\bar{\boldsymbol{q}}} + C(\boldsymbol{q},\dot{\boldsymbol{q}})\,T_r^{-1}\dot{\bar{\boldsymbol{q}}} + DT_r^{-1}\dot{\bar{\boldsymbol{q}}} + KT_r^{-1}\bar{\boldsymbol{q}} = L\boldsymbol{\tau}, \tag{6}$$

where $\ddot{\bar{\boldsymbol{q}}} = T_r\ddot{\boldsymbol{q}}$ and $\dot{\bar{\boldsymbol{q}}} = T_r\dot{\boldsymbol{q}}$, note that the vectors $\boldsymbol{q}$ and $\bar{\boldsymbol{q}}$ have the same elements but in different order, then : $\bar{M}(\boldsymbol{q}) = \bar{M}(\bar{\boldsymbol{q}})$ and $\bar{C}(\boldsymbol{q},\dot{\boldsymbol{q}}) = \bar{C}(\bar{\boldsymbol{q}},\dot{\bar{\boldsymbol{q}}})$.

Equation (6) is equivalent to the following expression:

$$\bar{M}(\boldsymbol{q})\,\ddot{\bar{\boldsymbol{q}}} + \bar{C}(\boldsymbol{q},\dot{\boldsymbol{q}})\,\dot{\bar{\boldsymbol{q}}} + \bar{D}\dot{\bar{\boldsymbol{q}}} + \bar{K}\bar{\boldsymbol{q}} = \bar{L}\boldsymbol{\tau}, \tag{7}$$

where $\bar{M}(\boldsymbol{q})_{2n\times 2n} = T_r M(\boldsymbol{q})\,T_r^{-1}$; $\bar{C}(\boldsymbol{q},\dot{\boldsymbol{q}})_{2n\times 2n} = T_r C(\boldsymbol{q},\dot{\boldsymbol{q}})\,T_r^{-1}$; $\bar{D}_{2n\times 2n} = T_r DT_r^{-1}$; $\bar{K}_{2n\times 2n} = T_r KT_r^{-1}$, $\bar{L}_{2n\times n} = T_r L$.

The dynamical model (7) can be written as follows:

$$\begin{bmatrix} \bar{M}_1^T(\boldsymbol{q}) \\ \vdots \\ \bar{M}_n^T(\boldsymbol{q}) \end{bmatrix} \begin{bmatrix} \ddot{\boldsymbol{q}}_1 \\ \vdots \\ \ddot{\boldsymbol{q}}_n \end{bmatrix} + \begin{bmatrix} \bar{C}_1^T(q,\dot{q}) \\ \vdots \\ \bar{C}_n^T(q,\dot{q}) \end{bmatrix} \begin{bmatrix} \dot{\boldsymbol{q}}_1 \\ \vdots \\ \dot{\boldsymbol{q}}_n \end{bmatrix} + \begin{bmatrix} \bar{D}_1^T \\ \vdots \\ \bar{D}_n^T \end{bmatrix} \begin{bmatrix} \dot{\boldsymbol{q}}_1 \\ \vdots \\ \dot{\boldsymbol{q}}_n \end{bmatrix} + \begin{bmatrix} \bar{K}_1^T \\ \vdots \\ \bar{K}_n^T \end{bmatrix} \begin{bmatrix} \boldsymbol{q}_1 \\ \vdots \\ \boldsymbol{q}_n \end{bmatrix} = \begin{bmatrix} \bar{L}_1 \\ \vdots \\ \bar{L}_n \end{bmatrix} \boldsymbol{\tau}, \tag{8}$$

where $\boldsymbol{q_i} = [q_{ri}\ \ q_{fi}]^T$; $\bar{M}_i^T = [\bar{M}_{i1}\ \ldots\ \bar{M}_{ii}\ \ldots\ \bar{M}_{in}]$; $\bar{C}_i^T = [\bar{C}_{i1}\ \ldots\ \bar{C}_{ii}\ \ldots\ \bar{C}_{in}]$

$$\bar{D}_i^T = \left[0_{2\times 2}\ \ldots\ 0_{2\times 2}\ \bar{D}_{ii}0_{2\times 2}\ \ldots\ 0_{2\times 2}\right];\quad \bar{K}_i^T = \left[0_{2\times 2}\ \ldots\ 0_{2\times 2}\ \bar{K}_{ii}0_{2\times 2}\ \ldots\ 0_{2\times 2}\right],$$

$$\bar{M}_{ii} = \begin{bmatrix} M_{ri} & M_{rfi} \\ M_{rfi} & M_{fi} \end{bmatrix};\quad \bar{C}_{ii} = \begin{bmatrix} C_{ri} & C_{rfi} \\ C_{rfi} & C_{fi} \end{bmatrix};\quad \bar{D}_{ii} = \begin{bmatrix} 0 & 0 \\ 0 & D_{fi} \end{bmatrix};\quad \bar{K}_{ii} = \begin{bmatrix} 0 & 0 \\ 0 & K_{fi} \end{bmatrix}.$$

The properties that will be used in the control law development can be deduced from the dynamical model of the flexible link manipulator and are given as follows:

P1: M, M_{rr}, M_{ff}, D_{ff} and K_{ff} are symmetric positive definite matrices.[20]

P2: The inertia-mass matrix $M(\boldsymbol{q})$ and the Coriolis matrix $C(\boldsymbol{q},\dot{\boldsymbol{q}})$ satisfy the following skew-symmetric property:

$$\boldsymbol{x}^T(\dot{M}(\boldsymbol{q},\dot{\boldsymbol{q}}) - 2C(\boldsymbol{q},\dot{\boldsymbol{q}}))\boldsymbol{x} = 0 \quad \forall \boldsymbol{x} \in \mathcal{R}^{n+z}. \tag{9}$$

https://doi.org/10.1017/S0263574714000459 Published online by Cambridge University Press

Let the desired trajectory associated to the rigid part of the *i*th subsystem, its first and second-order derivatives be $q_{ird}(t)$, $\dot{q}_{ird}(t)$, and $\ddot{q}_{ird}(t)$, respectively, and $q_{ifd}(t)$, $\dot{q}_{ifd}(t)$, and $\ddot{q}_{ifd}(t)$ are those associated to the flexible part of this subsystem. The objective is to track desired trajectories in the joint space and cancel vibration of the links. The desired positions of the flexible modes are then set to zero. Therefore, the desired trajectories must be carefully chosen so as to satisfy the control objective:

$$(q_{ir}, q_{if}) = (q_{ird}, 0). \tag{10}$$

3. Distributed Control Strategy

In this section, we present a distributed control strategy for *n*-flexible-link manipulator to track desired trajectories in the joint space while eliminating links' vibrations. The *n*-flexible-link system can be viewed as interconnected subsystems. Each subsystem has a pair of a joint and a flexible link. The distributed control strategy consists in controlling the *n*th subsystem while assuming that the remaining subsystems are stable. Then, the same strategy is applied backward to the $(n-1)$th subsystem and so on until the first subsystem.

3.1. Control law development

As mentioned earlier, the control strategy consists of controlling each subsystem backward from the last subsystem until the first one. Taking, for example, the *i*th subsystem, its equation of motion is derived from (8) as follows:

$$\bar{M}_i^T(\boldsymbol{q})\ddot{\bar{\boldsymbol{q}}} + \bar{C}_i^T(\boldsymbol{q}, \dot{\boldsymbol{q}})\dot{\bar{\boldsymbol{q}}} + \bar{D}_i^T\dot{\bar{\boldsymbol{q}}} + \bar{K}_i^T\bar{\boldsymbol{q}} = \bar{L}_i\boldsymbol{\tau}, \tag{11}$$

where $\bar{M}_i^T = [\,\bar{M}_{i1}\ \cdots\ \bar{M}_{ii}\ \ldots\ \bar{M}_{in}\,]^T$; $\bar{C}_i^T = [\,\bar{C}_{i1}\ \cdots\ \bar{C}_{ii}\ \ldots\ \bar{C}_{in}\,]^T$; $\bar{L}_i = \left[\begin{smallmatrix} 0\ \ldots\ 010\ \cdots\ 0 \\ 0\ \ldots\ 000\ \cdots\ 0 \end{smallmatrix}\right]_{2\times n}$ $\bar{D}_i^T = [\,\bar{D}_{i1}\ \cdots\ \bar{D}_{ii}\ \ldots\ \bar{D}_{in}\,]^T$; $\bar{K}_i^T = [\,\bar{K}_{i1}\ \cdots\ \bar{K}_{ii}\ \ldots\ \bar{K}_{in}\,]^T$; $\bar{M}_{ii} = \left[\begin{smallmatrix} M_{ri} & M_{rfi} \\ M_{rfi} & M_{fi} \end{smallmatrix}\right]$; $\bar{C}_{ii} = \left[\begin{smallmatrix} C_{ri} & C_{rfi} \\ C_{rfi} & C_{fi} \end{smallmatrix}\right]$; $\bar{D}_{ii} = \left[\begin{smallmatrix} 0 & 0 \\ 0 & D_{fi} \end{smallmatrix}\right]$; $\bar{K}_{ii} = \left[\begin{smallmatrix} 0 & 0 \\ 0 & K_{fi} \end{smallmatrix}\right]$. The *i*th subsystem is controlled by assuming that the remaining subsystems are stable. Then, we can define the new generalized coordinate as follows:

$$\bar{\mathbb{q}}_{\boldsymbol{i}} = [\,\boldsymbol{q_{d1}}\ \cdots\ \boldsymbol{q_{d(i-1)}}\ \boldsymbol{q_i}\ \boldsymbol{q_{d(i+1)}}\ \boldsymbol{q_{dn}}\,]^{\mathrm{T}} \tag{12}$$

where $\boldsymbol{q_{dj}} = [\,q_{rdj}\ q_{fdj}\,]$ and $\boldsymbol{q_i} = [\,q_{ri}\ q_{fi}\,]$ for $j = 1, \ldots, n, j \neq i$. Note that the rigid and flexible coordinates of the *i*th subsystem are the controlled ones and the rigid and flexible coordinates of the remaining subsystems are the desired ones. The velocity $\dot{\bar{\mathbb{q}}}_i$ is the time derivative of $\bar{\mathbb{q}}_i$ and the acceleration $\ddot{\bar{\mathbb{q}}}_i$ is the time derivative of $\dot{\bar{\mathbb{q}}}_i$. Using the new coordinate, the corresponding equation of motion is given as follows:

$$\bar{M}_i^T(\bar{\mathbb{q}}_i)\ddot{\bar{\mathbb{q}}}_i + \bar{C}_i^T(\bar{\mathbb{q}}_i, \dot{\bar{\mathbb{q}}}_i)\dot{\bar{\mathbb{q}}}_i + \bar{D}_i^T\dot{\bar{\mathbb{q}}}_i + \bar{K}_i^T\bar{\mathbb{q}}_i = \bar{L}_i\tau_i. \tag{13}$$

In other form, (13) can be written as:

$$\bar{M}_{ii}(\bar{\mathbb{q}}_i)\ddot{q}_i + \bar{C}_{ii}(\bar{\mathbb{q}}_i, \dot{\bar{\mathbb{q}}}_i)\dot{q}_i + \bar{D}_{ii}\dot{\boldsymbol{q}}_{\boldsymbol{i}} + \bar{K}_{ii}\boldsymbol{q_i} + \sum_{\substack{j=1 \\ j\neq i}}^{n} \bar{M}_{ij}(\bar{\mathbb{q}}_i)\ddot{\boldsymbol{q}}_{\boldsymbol{dj}} + \bar{C}_{ij}\left(\bar{\mathbb{q}}_i, \dot{\bar{\mathbb{q}}}i\right)\dot{\boldsymbol{q}}_{\boldsymbol{dj}} = \begin{bmatrix} \tau_i \\ 0 \end{bmatrix}. \tag{14}$$

Define the sliding surface of *i*th subsystem as follows:

$$\boldsymbol{s}_i = \begin{bmatrix} s_{ri} \\ s_{fi} \end{bmatrix} = \begin{bmatrix} \dot{e}_{ri} + \lambda_{ri}e_{ri} \\ \dot{e}_{fi} + \lambda_{fi}e_{fi} \end{bmatrix} = \begin{bmatrix} \dot{q}_{rdi} - \dot{q}_{ri} + \lambda_{ri}e_{ri} \\ \dot{q}_{fdi} - \dot{q}_{fi} + \lambda_{fi}e_{fi} \end{bmatrix}, \tag{15}$$

where $e_{ri} = q_{rdi} - q_{ri}$, and $e_{fi} = q_{fdi} - q_{fi}$ are the error signals and λ_{ri}, λ_{fi} are positive constants.

https://doi.org/10.1017/S0263574714000459 Published online by Cambridge University Press

The previous sliding surface can be written as follows:

$$\boldsymbol{s_i} = \begin{bmatrix} s_{ri} \\ s_{fi} \end{bmatrix} = \begin{bmatrix} \dot{u}_{ri} - \dot{q}_{ri} \\ \dot{u}_{fi} - \dot{q}_{fi} \end{bmatrix} = \dot{u}_i - \dot{q}_i, \tag{16}$$

where $\dot{u}_{ri} = \dot{q}_{rdi} + \lambda_{ri} e_{ri}$ and $\dot{u}_{fi} = \dot{q}_{fdi} + \lambda_{fi} e_{fi}$.

To control the ith subsystem, we propose the following control law:

$$\tau_i = T_i + v_{ri} - \delta\tau_{ri} \tag{17}$$

where v_{ri} is used for rigid part tracking, T_i is used to reduce the vibration of flexible part, and $\delta\tau_{ri}$ is the setting term

$$T_i = \begin{cases} \frac{s_{fi}(v_{fi}+\delta\tau_{fi})}{s_{ri}} \; ; \; s_{ri} \neq 0, \\ 0 \qquad\qquad\quad ; \; s_{ri} = 0, \end{cases} \tag{18}$$

$$\boldsymbol{v}_i = \begin{bmatrix} v_{ri} \\ v_{fi} \end{bmatrix} = \bar{M}_i^T(\bar{\mathbb{q}}_i)\ddot{\bar{\boldsymbol{u}}} + \bar{C}_i^T(\bar{\mathbb{q}}_i, \dot{\bar{\mathbb{q}}}_i)\dot{\bar{\boldsymbol{u}}} + \bar{D}_i^T\dot{\bar{\boldsymbol{u}}} + \bar{K}_i^T\bar{\boldsymbol{q}} + \bar{K}_{di}^T\bar{\boldsymbol{s}}, \tag{19}$$

$$\boldsymbol{\delta\tau_i} = \begin{bmatrix} \delta\tau_{ri} \\ \delta\tau_{fi} \end{bmatrix} = \delta\bar{M}_i^T\ddot{\bar{\boldsymbol{u}}} - \delta\bar{C}_i^T\dot{\bar{\boldsymbol{u}}}, \tag{20}$$

where $K_{di} \in \mathcal{R}^{2\times 2}$ is a diagonal positive matrix, $\delta\bar{M}_i^T = [\delta\bar{M}_{i1} \; \ldots \; \delta\bar{M}_{ii} \; \ldots \; \delta\bar{M}_{in}]_{2\times 2n}$; $\delta\bar{C}_i^T = [\delta\bar{C}_{i1} \; \ldots \; \delta\bar{C}_{ii} \; \ldots \; \delta\bar{C}_{in}]_{2\times 2n}$, and

$$\begin{aligned} \bar{\boldsymbol{u}} &= [\boldsymbol{u}_1 \; \cdots \; \boldsymbol{u_i} \; \cdots \; \boldsymbol{u_n}]^T = [u_{r1} \; u_{f1} \; \cdots u_{ri} \; u_{fi} \; \ldots u_{rn} \; u_{fn}]^T = T_r\boldsymbol{u}, \\ \bar{\boldsymbol{s}} &= [\boldsymbol{s}_1 \; \cdots \; \boldsymbol{s}_i \; \cdots \; \boldsymbol{s}_n]^T = [s_{r1} \; s_{f1} \; \cdots s_{ri} \; s_{fi} \; \ldots s_{rn} \; s_{fn}]^T = T_r\boldsymbol{s}, \end{aligned} \tag{21}$$

$$\delta\bar{M}_{ij} = \sum_{\substack{j=1 \\ j\neq i}}^{n} \frac{\partial\bar{M}_{ij}(\boldsymbol{q})}{\partial\boldsymbol{q_j}}\bigg|_{\boldsymbol{q}_{jd}} \tilde{\boldsymbol{q}}_j + R_{\bar{M}_{ij}}(\tilde{\boldsymbol{q}}_j), \tag{22}$$

$$\delta\bar{C}_{ij} = \sum_{\substack{j=1 \\ j\neq i}}^{n} \frac{\partial\bar{C}_{ij}(\boldsymbol{q}, \dot{\boldsymbol{q}})}{\partial\boldsymbol{q_j}}\bigg|_{\boldsymbol{q}_{jd}} \tilde{\boldsymbol{q}}_j + \sum_{\substack{j=1 \\ j\neq i}}^{n} \frac{\partial\bar{C}_{ij}(\boldsymbol{q}, \dot{\boldsymbol{q}})}{\partial\dot{\boldsymbol{q}}_j}\bigg|_{\boldsymbol{q}_{jd}} \dot{\tilde{\boldsymbol{q}}}_j + R_{\bar{C}_{ij}}(\tilde{\boldsymbol{q}}_j, \dot{\tilde{\boldsymbol{q}}}_j), \tag{23}$$

where $R_{\bar{M}_{ij}}$ and $R_{\bar{C}_{ij}}$ are the high-order terms of the Taylor series for $\bar{M}_{ij}(\boldsymbol{q})$ and $\bar{C}_{ij}(\boldsymbol{q})$, respectively[21] (see Appendix for more detail). The ith control law is shown by Fig. 2.

3.2. Stability analysis

This section presents the stability analysis of the error dynamics for all subsystems. The n control laws (17) can be written as follows:

$$\boldsymbol{\tau} = \boldsymbol{T} + \boldsymbol{v_r} - \boldsymbol{\delta\tau_r} \tag{24}$$

where $\boldsymbol{v_r} \in \Re^n$ is the first n elements of the vector $\boldsymbol{v}$, given in (19), while $\boldsymbol{v_f}$ are the remaining elements of $\boldsymbol{v}$. $\boldsymbol{T} \in \Re^n$ has T_i, given in (18), in the ith element.

The sliding surface for all subsystems can be written as follows:

$$\boldsymbol{s} = \begin{bmatrix} s_r \\ s_f \end{bmatrix} = \begin{bmatrix} \dot{e}_r + \lambda_r e_r \\ \dot{e}_f + \lambda_f e_f \end{bmatrix} = \begin{bmatrix} \dot{q}_{rd} - \dot{q}_r + \lambda_r e_r \\ \dot{q}_{fd} - \dot{q}_f + \lambda_f e_f \end{bmatrix} = \begin{bmatrix} \dot{u}_r - \dot{q}_r \\ \dot{u}_f - \dot{q}_f \end{bmatrix} = \dot{\boldsymbol{u}} - \dot{\boldsymbol{q}}. \tag{25}$$

https://doi.org/10.1017/S0263574714000459 Published online by Cambridge University Press

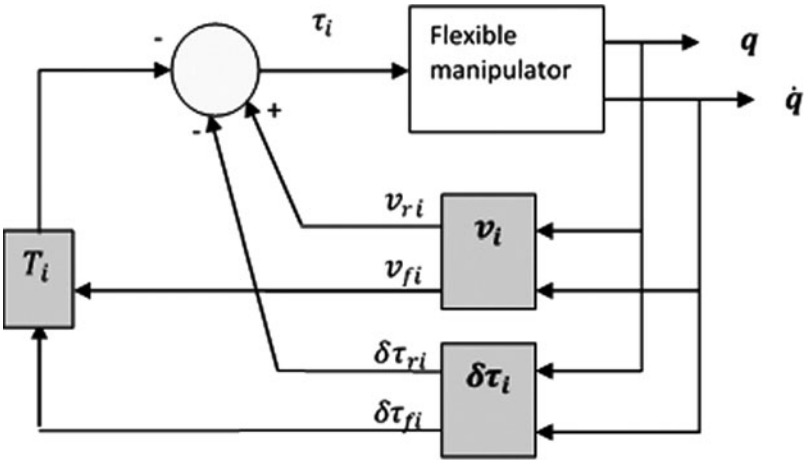


Fig. 2. The *i*th control law.

Using (25), the dynamical model (1) is given as follows:

$$M(\boldsymbol{q})(\ddot{\boldsymbol{u}} - \dot{\boldsymbol{s}}) + C(\boldsymbol{q}, \dot{\boldsymbol{q}})(\dot{\boldsymbol{u}} - \boldsymbol{s}) + D(\dot{\boldsymbol{u}} - \boldsymbol{s}) + K\boldsymbol{q} = L\boldsymbol{\tau}. \tag{26}$$

The error dynamics can be deduced as follows:

$$M(\boldsymbol{q})\dot{\boldsymbol{s}} + C(\boldsymbol{q}, \dot{\boldsymbol{q}})\boldsymbol{s} + D\boldsymbol{s} + K_d\boldsymbol{s} = M(\boldsymbol{q})\ddot{\boldsymbol{u}} + C(\boldsymbol{q}, \dot{\boldsymbol{q}})\dot{\boldsymbol{u}} + D\dot{\boldsymbol{u}} + K_d\boldsymbol{s} + K\boldsymbol{q} - L\boldsymbol{\tau}. \tag{27}$$

Proposition 1. *The error dynamics (27) is equivalent to the following expression:*

$$M(\boldsymbol{q})\dot{\boldsymbol{s}} + C(\boldsymbol{q}, \dot{\boldsymbol{q}})s + D\boldsymbol{s} + K_d\boldsymbol{s} = \begin{bmatrix} -\boldsymbol{T} \\ \boldsymbol{v}_f + \boldsymbol{\delta\tau}_f \end{bmatrix} \tag{28}$$

Proof: see Appendix.
For the stability analysis, let us define the following positive Lyapunov function:

$$V = \frac{1}{2}\boldsymbol{s}^T M(\boldsymbol{q})\boldsymbol{s}. \tag{29}$$

Take the time derivative of $V(t)$ to get

$$\dot{V}(t) = \boldsymbol{s}^T M\dot{\boldsymbol{s}} + \frac{1}{2}\boldsymbol{s}^T \dot{M}\boldsymbol{s}. \tag{30}$$

Using (28), $\dot{V}(t)$ becomes:

$$\begin{aligned}\dot{V}(t) &= \boldsymbol{s}^T\left(-C(\boldsymbol{q}, \dot{\boldsymbol{q}})\boldsymbol{s} - D\boldsymbol{s} - K_d\boldsymbol{s} + \begin{bmatrix} -T \\ \boldsymbol{v}_f + \boldsymbol{\delta\tau}_f \end{bmatrix}\right) + \frac{1}{2}s^T\dot{M}s \\ &= -\boldsymbol{s}^T(D + K_d)\boldsymbol{s} + \boldsymbol{s}^T\begin{bmatrix} -\boldsymbol{T} \\ \boldsymbol{v}_f + \boldsymbol{\delta\tau}_f \end{bmatrix}.\end{aligned}$$

Using the transformation matrix T_r, we can write:

$$\boldsymbol{s}^T\begin{bmatrix} -\boldsymbol{T} \\ \boldsymbol{v}_f + \boldsymbol{\delta\tau}_f \end{bmatrix} = \bar{\boldsymbol{s}}^T\bar{\boldsymbol{\tau}}_s, \tag{31}$$

https://doi.org/10.1017/S0263574714000459 Published online by Cambridge University Press

where $\boldsymbol{s}_i = \left[\begin{smallmatrix} s_{ri} \\ s_{fi} \end{smallmatrix}\right]$ and $\bar{\boldsymbol{\tau}}_{si} = \left[\begin{smallmatrix} -T_i \\ v_{fi} + \delta\tau_{fi} \end{smallmatrix}\right]$; $i = 1 \ldots n$.

$$\bar{\boldsymbol{s}}_{\boldsymbol{i}}^T \bar{\boldsymbol{\tau}}_{\boldsymbol{si}} = \begin{bmatrix} s_{ri} & s_{fi} \end{bmatrix} \begin{bmatrix} -T_i \\ v_{fi} + \delta\tau_{fi} \end{bmatrix} = -s_{ri} T_i + s_{fi}(v_{fi} + \delta\tau_{fi}). \tag{32}$$

Using (19), we can write:

$$\bar{\boldsymbol{s}}_{\boldsymbol{i}}^T \bar{\boldsymbol{\tau}}_{\boldsymbol{si}} = 0. \tag{33}$$

Using the transformation matrix T_r:

$$\boldsymbol{s}_{\boldsymbol{i}}^T \boldsymbol{\tau}_{\boldsymbol{si}} = 0. \tag{34}$$

Then,

$$\boldsymbol{s}^T \begin{bmatrix} -\boldsymbol{T} \\ \boldsymbol{v}_f + \boldsymbol{\delta\tau}_f \end{bmatrix} = \sum_{i=1}^{n} \boldsymbol{s}_{\boldsymbol{i}}^T \boldsymbol{\tau}_{\boldsymbol{si}} = 0. \tag{35}$$

Then, the time derivative of $V(t)$ becomes:

$$\dot{V}(t) = -\boldsymbol{s}^T (D + K_d)\, \boldsymbol{s}. \tag{36}$$

Because D and K_d are positive-definite diagonal matrices, then $\dot{V}(t)$ is negative. Using Barbalat lemma,[22] the error dynamics is globally asymptotically stable.

4. Application to Two-Flexible-Link Manipulator

4.1. System description

In this section, the control strategy presented in the previous sections is tested on the 2-DOF Serial Flexible Link robot (Fig. 3) manufactured by Quanser. It consists of two motors, two flexible links, and a payload. It moves in the horizontal plane and is connected by rigid revolute joints. The system is actuated by two torques generated by the motors. The ith motor has an angle q_{ri} and the i-th flexible link, supposed uniform, has a mass m_i and length L_i, linear density ρ_i, and rigidity EI_i. m_p is the mass of the payload. The second link is attached to the rotor of the second motor and the first link is attached to the first motor. Axes (X_1, Y_1) for link 1 and (X_2, Y_2) for link 2, move with the corresponding links. $\left(\hat{X}_0, \hat{Y}_0\right)$ is the fixed reference frame. The deformations of the links are assumed to be small and the flexible links are modeled as Euler-Bernoulli beams.

In this section, the two-flexible-link model given in refs. [22, 23] is modified by only considering the first flexible mode of each link (see Appendix). Then, we have $n = 2$, $z = 2$ and $z_1 = z_2 = 1$.

The dynamical model of the two-flexible-link manipulator is given by:

$$M(q)\,\ddot{\boldsymbol{q}} + C(q, \dot{q})\,\dot{\boldsymbol{q}} + D\dot{\boldsymbol{q}} + K\boldsymbol{q} = L\boldsymbol{\tau}, \tag{37}$$

where

$$M = \begin{bmatrix} M_{11} & M_{12} & M_{13} & M_{14} \\ M_{21} & M_{22} & M_{23} & M_{24} \\ M_{31} & M_{32} & M_{33} & M_{34} \\ M_{41} & M_{42} & M_{43} & M_{44} \end{bmatrix}; C = \begin{bmatrix} C_{11} & C_{12} & C_{13} & C_{14} \\ C_{21} & C_{22} & C_{23} & C_{24} \\ C_{31} & C_{32} & C_{33} & C_{34} \\ C_{41} & C_{42} & C_{43} & C_{44} \end{bmatrix}; D = \begin{bmatrix} 0 & 0 & 0 & 0 \\ 0 & 0 & 0 & 0 \\ 0 & 0 & D_{f1} & 0 \\ 0 & 0 & 0 & D_{f2} \end{bmatrix};$$

https://doi.org/10.1017/S0263574714000459 Published online by Cambridge University Press

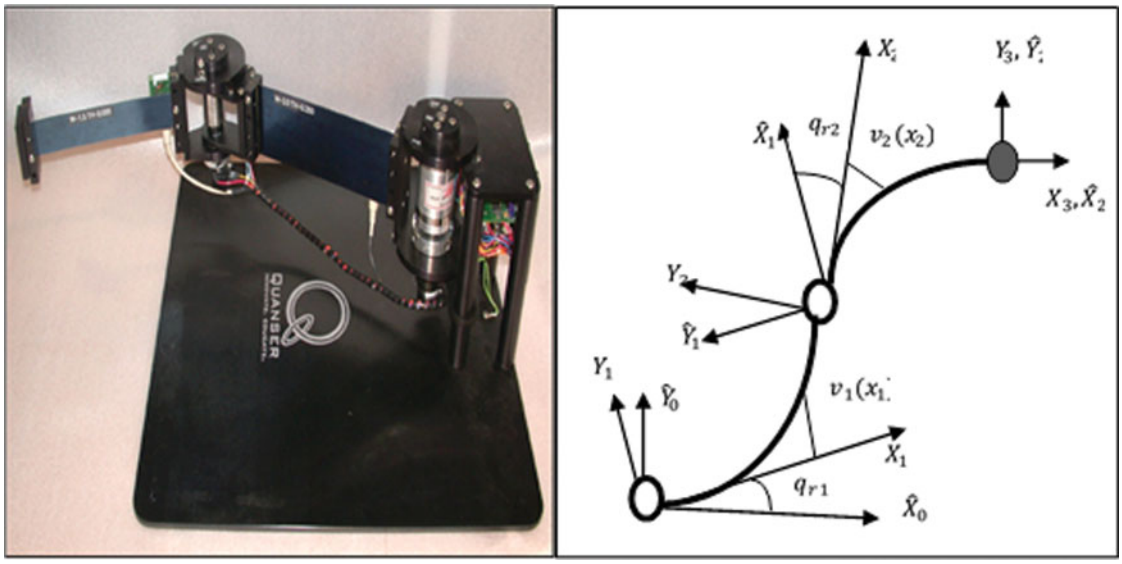


Fig. 3. Two-flexible-link manipulator.

$$K = \begin{bmatrix} 0 & 0 & 0 & 0 \\ 0 & 0 & 0 & 0 \\ 0 & 0 & K_{f1} & 0 \\ 0 & 0 & 0 & K_{f2} \end{bmatrix}, q = \begin{bmatrix} q_{r1} \\ q_{r2} \\ q_{f1} \\ q_{f2} \end{bmatrix}, L = \begin{bmatrix} 1 & 0 \\ 0 & 1 \\ 0 & 0 \\ 0 & 0 \end{bmatrix}, \text{and } \boldsymbol{\tau} = \begin{bmatrix} \tau_1 \\ \tau_2 \end{bmatrix}.$$

As in (3), we can write:

$$M_r = \begin{bmatrix} M_{11} & M_{12} \\ M_{21} & M_{22} \end{bmatrix}; M_{rf} = \begin{bmatrix} M_{13} & M_{14} \\ M_{23} & M_{24} \end{bmatrix}; M_f = \begin{bmatrix} M_{33} & M_{34} \\ M_{43} & M_{44} \end{bmatrix}; C_{rr} = \begin{bmatrix} C_{11} & C_{12} \\ C_{21} & C_{22} \end{bmatrix};$$
$$C_{rf} = \begin{bmatrix} C_{13} & C_{14} \\ C_{23} & C_{24} \end{bmatrix}; C_{ff} = \begin{bmatrix} C_{33} & C_{34} \\ C_{43} & C_{44} \end{bmatrix}; D_f = \begin{bmatrix} D_{f1} & 0 \\ 0 & D_{f2} \end{bmatrix}, \text{ and } K_f = \begin{bmatrix} K_{f1} & 0 \\ 0 & K_{f2} \end{bmatrix}.$$

For two flexiblelinks, the corresponding transformation matrix (5) becomes,

$$T_r = \begin{bmatrix} 1 & 0 & 0 & 0 \\ 0 & 0 & 1 & 0 \\ 0 & 1 & 0 & 0 \\ 0 & 0 & 0 & 1 \end{bmatrix}. \tag{38}$$

Using the matrix of transformation (38), the dynamical model (37) is equivalent to the following equation:

$$\bar{M}(\boldsymbol{q})\ddot{\bar{\boldsymbol{q}}} + \bar{C}(\boldsymbol{q}, \dot{\boldsymbol{q}})\dot{\bar{\boldsymbol{q}}} + \bar{D}\dot{\bar{\boldsymbol{q}}} + \bar{K}\bar{q} = \bar{L}\tau, \tag{39}$$

where

$$\bar{M} = \begin{bmatrix} M_{11} & M_{13} & M_{12} & M_{14} \\ M_{31} & M_{33} & M_{32} & M_{34} \\ M_{21} & M_{23} & M_{22} & M_{24} \\ M_{41} & M_{43} & M_{42} & M_{44} \end{bmatrix}; \bar{C} = \begin{bmatrix} C_{11} & C_{13} & C_{12} & C_{14} \\ C_{31} & C_{33} & C_{32} & C_{34} \\ C_{21} & C_{23} & C_{22} & C_{24} \\ C_{41} & C_{43} & C_{42} & C_{44} \end{bmatrix}; \bar{D} = \begin{bmatrix} 0 & 0 & 0 & 0 \\ 0 & D_{f1} & 0 & 0 \\ 0 & 0 & 0 & 0 \\ 0 & 0 & 0 & D_{f2} \end{bmatrix};$$

https://doi.org/10.1017/S0263574714000459 Published online by Cambridge University Press

$$\bar{K} = \begin{bmatrix} 0 & 0 & 0 & 0 \\ 0 & K_{f1} & 0 & 0 \\ 0 & 0 & 0 & 0 \\ 0 & 0 & 0 & K_{f2} \end{bmatrix}; \bar{\boldsymbol{q}} = \begin{bmatrix} q_1 \\ q_2 \end{bmatrix} = \begin{bmatrix} q_{r1} \\ q_{f1} \\ q_{r2} \\ q_{f2} \end{bmatrix}; \bar{L} = \begin{bmatrix} 1 & 0 \\ 0 & 0 \\ 0 & 1 \\ 0 & 0 \end{bmatrix}, \text{and } \boldsymbol{\tau} = \begin{bmatrix} \tau_1 \\ \tau_2 \end{bmatrix}$$

In the two subsystems form, (39) can be written as:

$$\begin{bmatrix} \bar{M}_{11} & \bar{M}_{12} \\ \bar{M}_{21} & \bar{M}_{22} \end{bmatrix} \begin{bmatrix} \ddot{\boldsymbol{q}}_1 \\ \ddot{\boldsymbol{q}}_2 \end{bmatrix} + \begin{bmatrix} \bar{C}_{11} & \bar{C}_{12} \\ \bar{C}_{21} & \bar{C}_{22} \end{bmatrix} \begin{bmatrix} \dot{q}_1 \\ \dot{q}_2 \end{bmatrix} + \begin{bmatrix} \bar{D}_{11} & \bar{D}_{12} \\ \bar{D}_{21} & \bar{D}_{22} \end{bmatrix} \begin{bmatrix} \dot{q}_1 \\ \dot{q}_2 \end{bmatrix} + \begin{bmatrix} \bar{K}_{11} & \bar{K}_{12} \\ \bar{K}_{21} & \bar{K}_{22} \end{bmatrix} \begin{bmatrix} \boldsymbol{q}_1 \\ \boldsymbol{q}_2 \end{bmatrix} = \begin{bmatrix} \bar{L}_1 \boldsymbol{\tau} \\ \bar{L}_2 \boldsymbol{\tau} \end{bmatrix} \tag{40}$$

where

$$\bar{M}_{11} = \begin{bmatrix} M_{11} & M_{13} \\ M_{31} & M_{33} \end{bmatrix}; \bar{M}_{12} = \begin{bmatrix} M_{12} & M_{14} \\ M_{32} & M_{34} \end{bmatrix}; \bar{C}_{11} = \begin{bmatrix} C_{11} & C_{13} \\ C_{31} & C_{33} \end{bmatrix}; \bar{C}_{12} = \begin{bmatrix} C_{12} & C_{14} \\ C_{32} & C_{34} \end{bmatrix};$$

$$\bar{D}_{11} = \begin{bmatrix} 0 & 0 \\ 0 & D_{f1} \end{bmatrix}; \bar{D}_{12} = \begin{bmatrix} 0 & 0 \\ 0 & 0 \end{bmatrix}; \bar{K}_{11} = \begin{bmatrix} 0 & 0 \\ 0 & K_{f1} \end{bmatrix}; \bar{K}_{12} = \begin{bmatrix} 0 & 0 \\ 0 & 0 \end{bmatrix}; \bar{M}_{21} = \begin{bmatrix} M_{21} & M_{23} \\ M_{41} & M_{43} \end{bmatrix};$$

$$\bar{M}_{22} = \begin{bmatrix} M_{22} & M_{24} \\ M_{42} & M_{44} \end{bmatrix}; \bar{C}_{21} = \begin{bmatrix} C_{21} & C_{23} \\ C_{41} & C_{43} \end{bmatrix}; \bar{C}_{22} = \begin{bmatrix} C_{22} & C_{24} \\ C_{42} & C_{44} \end{bmatrix}; \bar{D}_{21} = \begin{bmatrix} 0 & 0 \\ 0 & 0 \end{bmatrix}; \bar{D}_{22} = \begin{bmatrix} 0 & 0 \\ 0 & D_{f2} \end{bmatrix};$$

$$\bar{K}_{21} = \begin{bmatrix} 0 & 0 \\ 0 & 0 \end{bmatrix}; \bar{K}_{22} = \begin{bmatrix} 0 & 0 \\ 0 & K_{f2} \end{bmatrix}; \boldsymbol{q}_1 = \begin{bmatrix} q_{r1} \\ q_{f1} \end{bmatrix}; \boldsymbol{q}_2 = \begin{bmatrix} q_{r2} \\ q_{f2} \end{bmatrix}; \bar{L}_1 = \begin{bmatrix} 1 & 0 \\ 0 & 0 \end{bmatrix}; \bar{L}_2 = \begin{bmatrix} 0 & 1 \\ 0 & 0 \end{bmatrix}.$$

Equation (40) can be written in the following form that will be used for the control law:

$$\begin{bmatrix} \bar{M}_1^T \\ \bar{M}_2^T \end{bmatrix} \ddot{\bar{\boldsymbol{q}}} + \begin{bmatrix} \bar{C}_1^T \\ \bar{C}_2^T \end{bmatrix} \dot{\bar{\boldsymbol{q}}} + \begin{bmatrix} \bar{D}_1^T \\ \bar{D}_2^T \end{bmatrix} \dot{\bar{\boldsymbol{q}}} + \begin{bmatrix} \bar{K}_1^T \\ \bar{K}_2^T \end{bmatrix} \bar{\boldsymbol{q}} = \begin{bmatrix} \bar{L}_1 \tau_1 \\ \bar{L}_2 \tau_2 \end{bmatrix}, \tag{41}$$

where $\bar{M}_1^T = [\,\bar{M}_{11}\ \bar{M}_{12}\,]$; $\bar{C}_1^T = [\,\bar{C}_{11}\ \bar{C}_{12}\,]$; $\bar{D}_1^T = [\,\bar{D}_{11}\ \bar{D}_{12}\,]$; $\bar{K}_1^T = [\,\bar{K}_{11}\ \bar{K}_{12}\,]$; $\bar{M}_2^T = [\,\bar{M}_{21}\ \bar{M}_{22}\,]$; $\bar{C}_2^T = [\,\bar{C}_{21}\ \bar{C}_{22}\,]$; $\bar{D}_2^T = [\,\bar{D}_{21}\ \bar{D}_{22}\,]$; $\bar{K}_2^T = [\,\bar{K}_{21}\ \bar{K}_{22}\,]$.

4.2. Distributed control law

For a two-flexible-link manipulator, the control law is developed in two steps. The first consists of developing the control law for the second subsystem (second joint and link) by assuming that the first subsystem is stable. In the second step, we develop the control law for the first subsystem using the same strategy.

Starting now by the last subsystem, the generalized rigid and flexible coordinates are given by:

$$\bar{\mathbb{q}}_2 = \begin{bmatrix} \boldsymbol{q}_{\boldsymbol{d}1} & \boldsymbol{q}_2 \end{bmatrix}^T = \begin{bmatrix} q_{rd1} & q_{fd1} & q_{r2} & q_{f2} \end{bmatrix}^{\mathrm{T}}. \tag{42}$$

Note that, for the first subsystem, the rigid and flexible coordinates are the desired coordinates and for the second subsystem they are the controlled ones.

According to dynamical model (41), the equation of motion of the second link is given by:

$$\bar{M}_2^T(\bar{\mathbb{q}}_2)\ddot{\bar{q}}_2 + \bar{C}_2^T(\bar{\mathbb{q}}_2, \dot{\bar{\mathbb{q}}}_2)\dot{\bar{\mathbb{q}}}_2 + \bar{\mathbb{q}} D_2^T \dot{\bar{\mathbb{q}}}_2 + \bar{K}_2^T \bar{\mathbb{q}}_2 = \bar{L}_2 \boldsymbol{\tau} = \begin{bmatrix} \tau_2 \\ 0 \end{bmatrix}. \tag{43}$$

The control law proposed for the second subsystem is given by the following equation:

$$\tau_2 = T_2 + v_{r2} - \delta\tau_{r2}, \tag{44}$$

https://doi.org/10.1017/S0263574714000459 Published online by Cambridge University Press

where

$$T_2 = \begin{cases} \frac{s_{f2}\left(v_{f2}+\delta\tau_{f2}\right)}{s_{r2}} & ; s_{r2} \neq 0, \\ 0 & ; s_{r2} = 0, \end{cases} \tag{45}$$

$$\boldsymbol{v}_2 = \begin{bmatrix} v_{r2} \\ v_{f2} \end{bmatrix} = \bar{M}_2^T\left(\bar{\mathbb{q}}_2\right)\ddot{\bar{\boldsymbol{u}}} + \bar{C}_2^T\left(\bar{\mathbb{q}}_2, \dot{\bar{\mathbb{q}}}_2\right)\dot{\bar{\boldsymbol{u}}} + \bar{D}_2^T\dot{\bar{\boldsymbol{u}}} + \bar{K}_2^T\bar{\boldsymbol{q}} + \bar{K}_{d2}^T\bar{\boldsymbol{s}}, \tag{46}$$

$$\boldsymbol{\delta\tau}_2 = \begin{bmatrix} \delta\tau_{r2} \\ \delta\tau_{f2} \end{bmatrix} = \delta M_2^T\ddot{\bar{\boldsymbol{u}}} - \delta C_2^T\dot{\bar{\boldsymbol{u}}}, \tag{47}$$

where $\bar{K}_2^T = \left[\begin{smallmatrix} 0 & 0 & K_{d2r} & 0 \\ 0 & 0 & 0 & K_{d2f} \end{smallmatrix}\right]$; K_{d2r} and K_{d2f} are positive constants.

$$\dot{\bar{\boldsymbol{u}}} = [\,\dot{\boldsymbol{u}}_1 \quad \dot{\boldsymbol{u}}_2\,]^T = [\,\dot{u}_{1r} \quad \dot{u}_{1f} \quad \dot{u}_{2r} \quad \dot{u}_{2f}\,]^T = T_r\dot{\boldsymbol{u}};\ \boldsymbol{u} = [\,\dot{u}_{1r} \quad \dot{u}_{2r} \quad \dot{u}_{1f} \quad \dot{u}_{2f}\,]^T;$$

$$\bar{\boldsymbol{s}} = [\,\boldsymbol{s}_1 \quad \boldsymbol{s}_2\,]^T = [\,s_{1r} \quad s_{1f} \quad s_{2r} \quad s_{2f}\,]^{\mathrm{T}} = T_r\boldsymbol{s};\ \boldsymbol{s} = [\,s_{1r} \quad s_{2r} \quad s_{1f} \quad s_{2f}\,]^{\mathrm{T}},$$

$$\delta\bar{M}_2^T = [\delta\bar{M}_{21}\ \delta\bar{M}_{22}];\ \delta\bar{C}_2^{\mathrm{T}} = [\delta\bar{C}_{21}\ \delta\bar{C}_{22}]$$

$$\delta M_{ij} = \left.\frac{\partial M_{ij}(\boldsymbol{q})}{\partial q_1}\right|_{\boldsymbol{q}_{1d}}\tilde{\boldsymbol{q}}_1 + R_{M_{ij}}(\tilde{\boldsymbol{q}}_1); \delta C_{ij} = \left.\frac{\partial C_{ij}(\boldsymbol{q},\dot{\boldsymbol{q}})}{\partial \boldsymbol{q}_1}\right|_{q_{1d}}\tilde{\boldsymbol{q}}_1 + \left.\frac{\partial C_{ij}(\boldsymbol{q},\dot{\boldsymbol{q}})}{\partial \dot{\boldsymbol{q}}_1}\right|_{\boldsymbol{q}_{1d}}\dot{\tilde{\boldsymbol{q}}}_1 + R_{C_{ij}}(\tilde{\boldsymbol{q}}_1)$$

$R_{M_{ij}}$ and $R_{C_{ij}}$ are the high-order terms of the Taylor series for $M_{ij}(\boldsymbol{q})$ and $C_{ij}(\boldsymbol{q},\dot{\boldsymbol{q}})$, respectively.

Proceeding to the first subsystem and developing the control law assuming that the second subsystem is stable, the equation of motion of the first subsystem is given by:

$$\bar{M}_1^T(\bar{\mathbb{q}}_1)\ddot{\bar{\mathbb{q}}}_1 + \bar{C}_1^T(\bar{\mathbb{q}}_1,\dot{\bar{\mathbb{q}}}_1)\dot{\bar{\mathbb{q}}}_1 + \bar{D}_1^T\dot{\bar{\mathbb{q}}}_1 + \bar{K}_1^T\bar{\mathbb{q}}_1 = \bar{L}_1\boldsymbol{\tau} = \begin{bmatrix} \tau_1 \\ 0 \end{bmatrix} \tag{48}$$

where

$$\bar{\mathbb{q}}_1 = [\,\boldsymbol{q}_1 \quad \boldsymbol{q}_{d2}\,]^T = [\,q_{r1} \quad q_{f1} \quad q_{rd2} \quad q_{fd2}\,]^{\mathrm{T}}. \tag{49}$$

The control law is given by:

$$\tau_1 = T_1 + v_{r1} - \delta\tau_{r1}, \tag{50}$$

where

$$T_1 = \begin{cases} \frac{s_{f1}\left(v_{f1}+\delta\tau_{f1}\right)}{s_{r1}} & ; s_{r1} \neq 0, \\ 0 & ; s_{r1} = 0, \end{cases} \tag{51}$$

$$\boldsymbol{v}_1 = \begin{bmatrix} v_{r1} \\ v_{f1} \end{bmatrix} = \bar{M}_1^T\left(\bar{\mathbb{q}}_1\right)\ddot{\bar{\boldsymbol{u}}} + \bar{C}_1^T(\bar{\mathbb{q}}_1,\dot{\bar{\mathbb{q}}}_1)\dot{\bar{\boldsymbol{u}}} + \bar{D}_1^T\dot{\bar{u}} + \bar{K}_1^T\bar{\boldsymbol{q}} + \bar{K}_{d1}^T\bar{\boldsymbol{s}}, \tag{52}$$

$$\boldsymbol{\delta\tau}_1 = \begin{bmatrix} \delta\tau_{r1} \\ \delta\tau_{f1} \end{bmatrix} = \delta M_1^T\ddot{\bar{\boldsymbol{u}}} - \delta C_1^T\dot{\bar{\boldsymbol{u}}}, \tag{53}$$

where $K_{d1} = \left[\begin{smallmatrix} 0 & 0 & K_{d1r} & 0 \\ 0 & 0 & 0 & K_{d1f} \end{smallmatrix}\right]$; K_{d1r} and K_{d1f} are positive constants,

$$\delta\bar{M}_1^T = \left[\delta\bar{M}_{11}\ \delta\bar{M}_{12}\right]_{2\times 4};\ \delta\bar{C}_1^T = \left[\delta\bar{C}_{11}\ \delta\bar{C}_{12}\right]_{2\times 4}.$$

$$\delta M_{ij} = \left.\frac{\partial M_{ij}(\boldsymbol{q})}{\partial \boldsymbol{q}_2}\right|_{q_{2d}}\tilde{\boldsymbol{q}}_2 + R_{M_{ij}}(\tilde{\boldsymbol{q}}_2); \delta C_{ij} = \left.\frac{\partial C_{ij}(q,q)}{\partial q_2}\right|_{q_{2d}}\tilde{\boldsymbol{q}}_2 + \left.\frac{\partial C_{ij}(\boldsymbol{q},\dot{\boldsymbol{q}})}{\partial \dot{\boldsymbol{q}}_2}\right|_{\mathbf{q_{2d}}}\dot{\tilde{\boldsymbol{q}}}_2 + R_{C_{ij}}(\tilde{\boldsymbol{q}}_2)$$

$R_{\bar{M}1j}$ and $R_{\bar{C}1j}$ are the high-order terms of the Taylor series for $\bar{M}_{2j}(\boldsymbol{q})$and $\bar{C}_{2j}(q,\dot{\boldsymbol{q}})$, respectively.

https://doi.org/10.1017/S0263574714000459 Published online by Cambridge University Press

Table I. System physical parameters.

Parameter	Link 1	Link 2
Link length (L_i)	0.202 m	0.2 m
Elasticity	2.068 10^{11} N/m^2	2.068 10^{11} N/m^2
Link moment of inertia	0.17 kg m^2	0.0064 10^{-6} kg m^2
Gear ratio	100	50
Rotor moment of inertia	6.28 10^{-6} kg m^2	1.03 10^{-6} kg m^2
Drive moment of inertia	7.63 10^{-4} kg m^2	44.55 10^{-6} kg m^2
Drive Torque constant	0.119 Nm/A	0.0234 Nm/A
Maximum Rotation	$\pm$ 90 deg	$\pm$ 90 deg

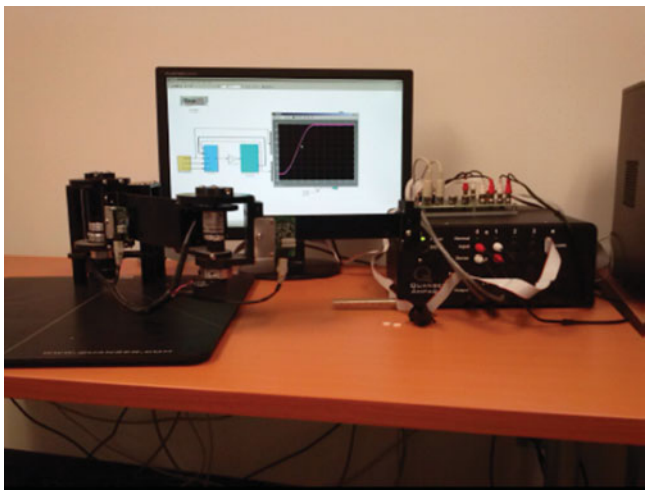


Fig. 4. Quanser two link flexible robot.

4.3. Experimental results

The parameters of the 2-DOF Serial Flexible Link robot (Fig. 4) are given in Table I.

The experimental setup of the two link serial flexible manipulator robot is shown in Figs. 4 and 5.

The main components of the setup are: a linear amplifier, Q8 terminal board, DAQ system, sensors, such as strain gauges, encoder, and limit switches. The interface between the computer and the setup is the Quanser Q8 data acquisition board. Simulink with Real-Time Workshop (RTW) of Mathworks® is used for real-time implementation of the proposed controllers. Q8 software is used to transform the data from the computer to the system, which allows the SIMULINK models to run in real-time target. The torque input provided by the control algorithm is sent to the robot trough Q8 data acquisition and the linear current amplifier. A current sensor measures the current of each actuator.

The desired trajectory of the joint takes up a polynomial function given by the following expressions:[24]

$$q_{rd1}(t) = a_{10} + a_{11}t + a_{12}t^2 + a_{13}t^3 + a_{14}t^4 + a_{15}t^5, \tag{54}$$

$$q_{rd2}(t) = a_{20} + a_{21}t + a_{22}t^2 + a_{23}t^3 + a_{24}t^4 + a_{25}t^5, \tag{55}$$

$$q_{fd1}(t) = q_{fd2}(t) = 0,$$

for $0 \leq t \leq T_f = 5s$. For $t \geq T_f$, $q_{rd1}(t) = \frac{\pi}{4}$ and $q_{rd2}(t) = \frac{\pi}{8}$.

The desired trajectories are given in Fig. 6.

The shape function of each link is given in ref. [20]. Using the system parameters, the shape functions evaluated at the extremity of the links and their derivative are given as follows: $\emptyset_{1L} = 0.39$, $\emptyset_{2L} = 1.49$, $\emptyset'_{1L} = 1.34$, and $\emptyset'_{2L} = 4.3$.

https://doi.org/10.1017/S0263574714000459 Published online by Cambridge University Press

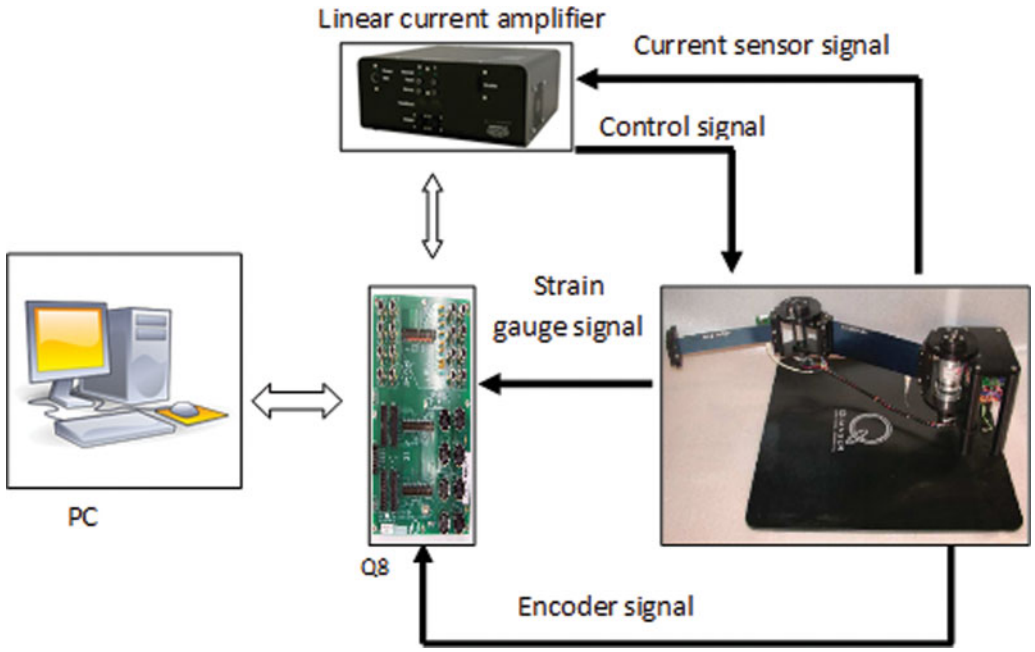


Fig. 5. Real-Time setup.

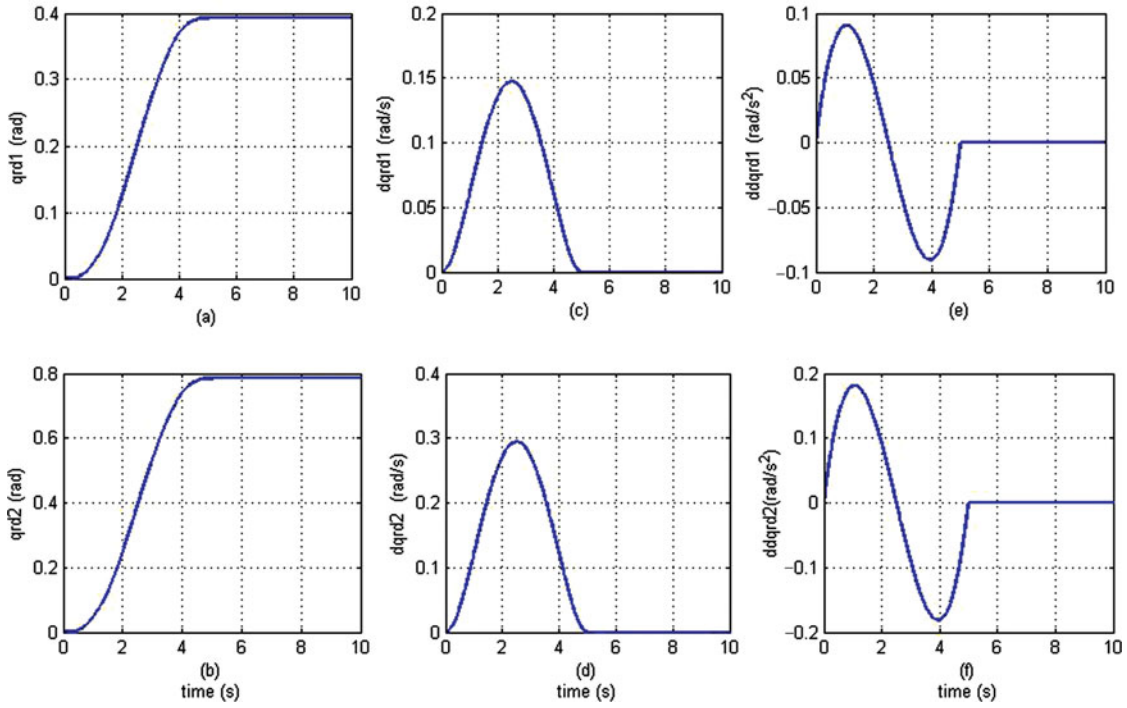


Fig. 6. Desired trajectories: (a)–(b) position, (c)–(d) velocity, (e)–(f) acceleration of rigid part.

The controller's gains are chosen using a trial and error method as follows: For the distributed control strategy, the selected gains are: $K_{d1r} = 15$; $K_{d1f} = 10$, $K_{d2r} = 25$ and $K_{d2f} = 10$.

The previous theoretical development of the control law that ensures the global stability is given in the general case, i.e. for any high order in the Taylor series. In the real-time implementation, a finite order is fixed. In this section, and for simplicity, the Taylor series is limited to the first order. Then, $R_{M_{ij}} = R_{C_{ij}} = 0$.

The experimental results for the distributed control are shown in Figs. 7–9.

https://doi.org/10.1017/S0263574714000459 Published online by Cambridge University Press

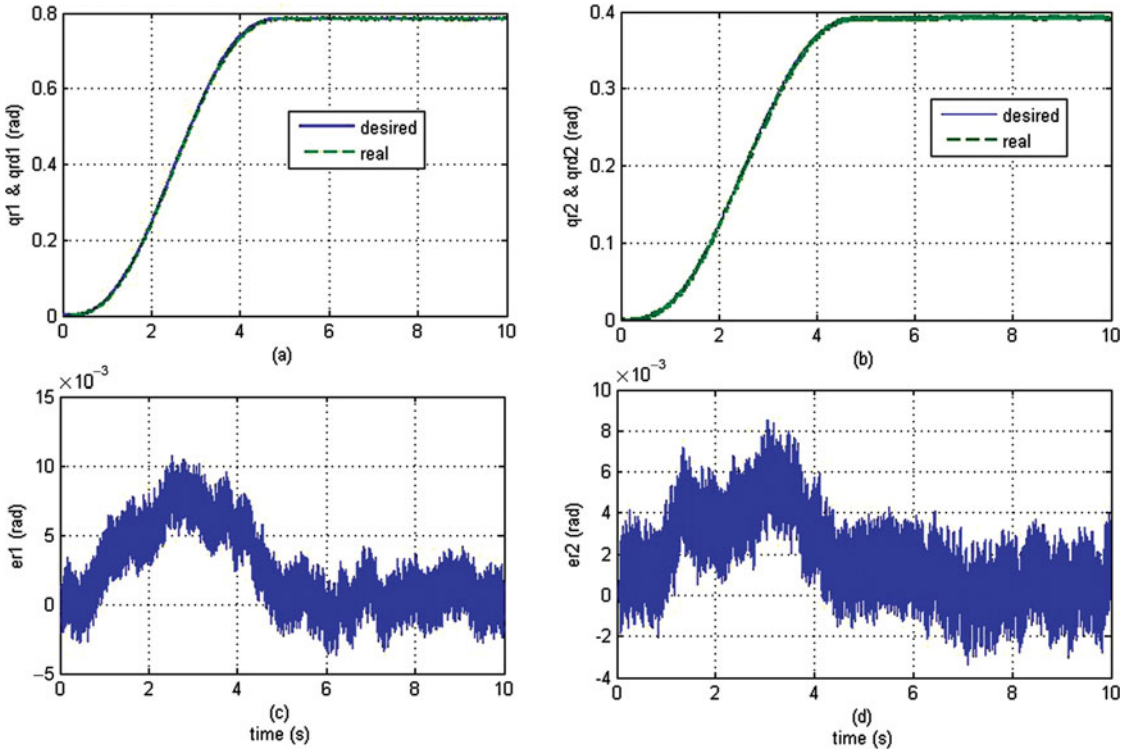


Fig. 7. Distributed control: (a)–(b) joint tracking trajectories, (c)–(d) joint tracking errors.

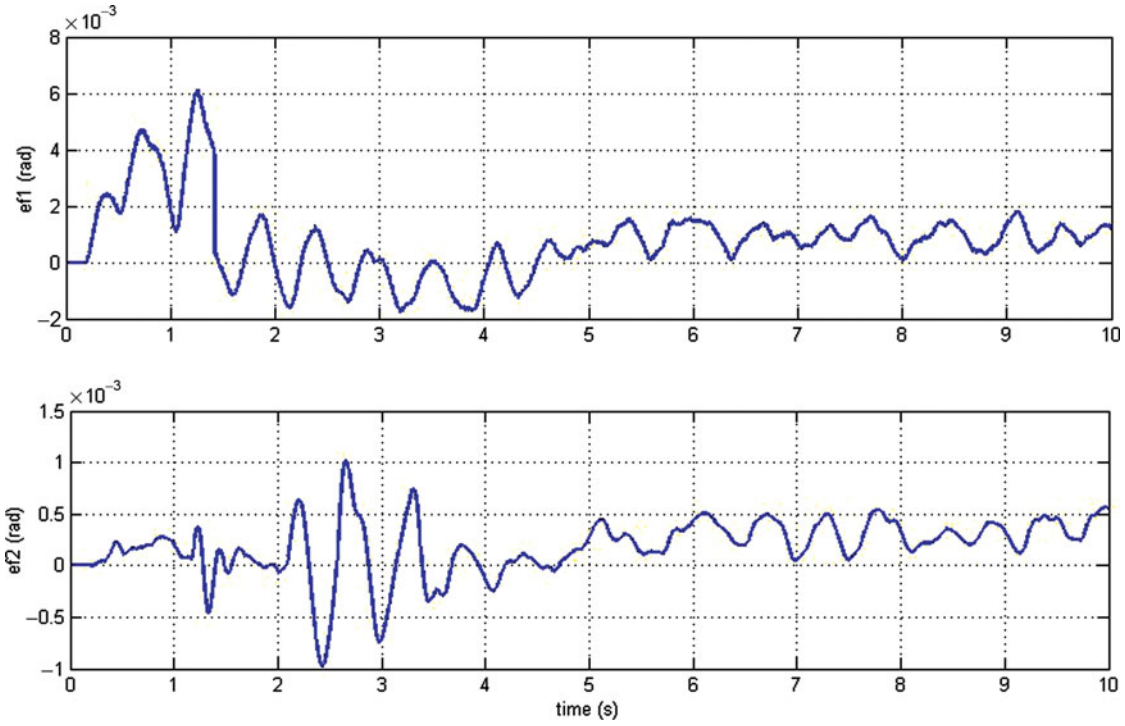


Fig. 8. Distributed control: errors of flexible parts.

https://doi.org/10.1017/S0263574714000459 Published online by Cambridge University Press

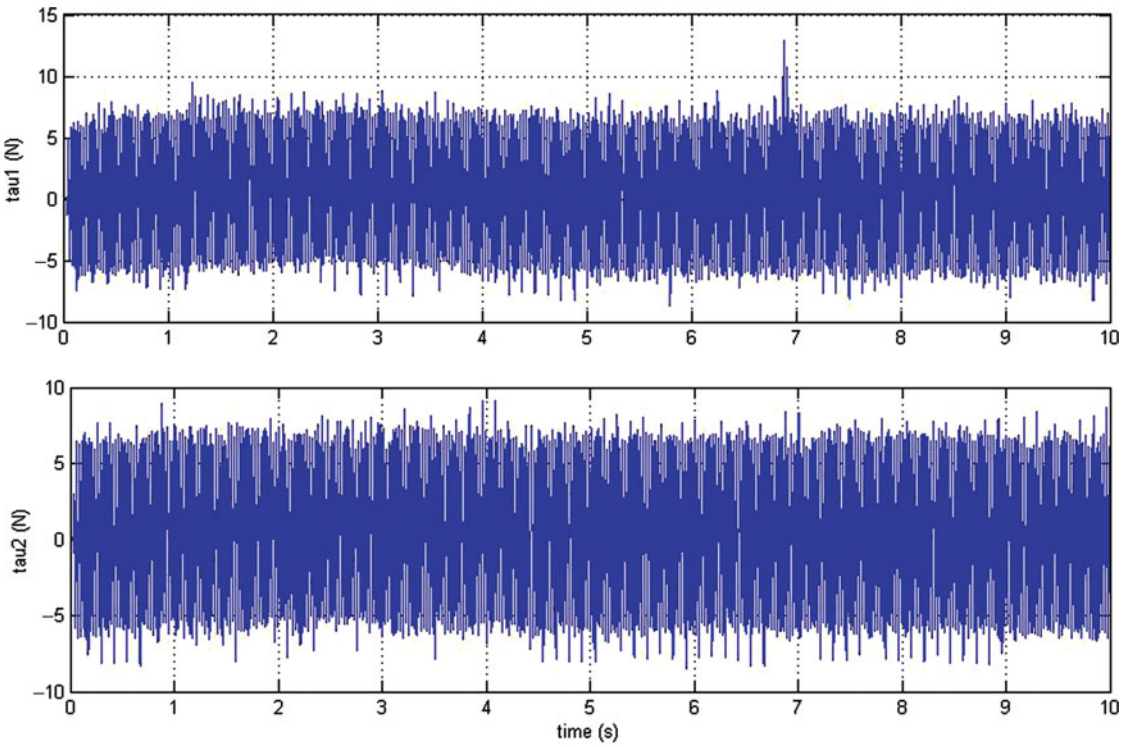


Fig. 9. Distributed control: input torque.

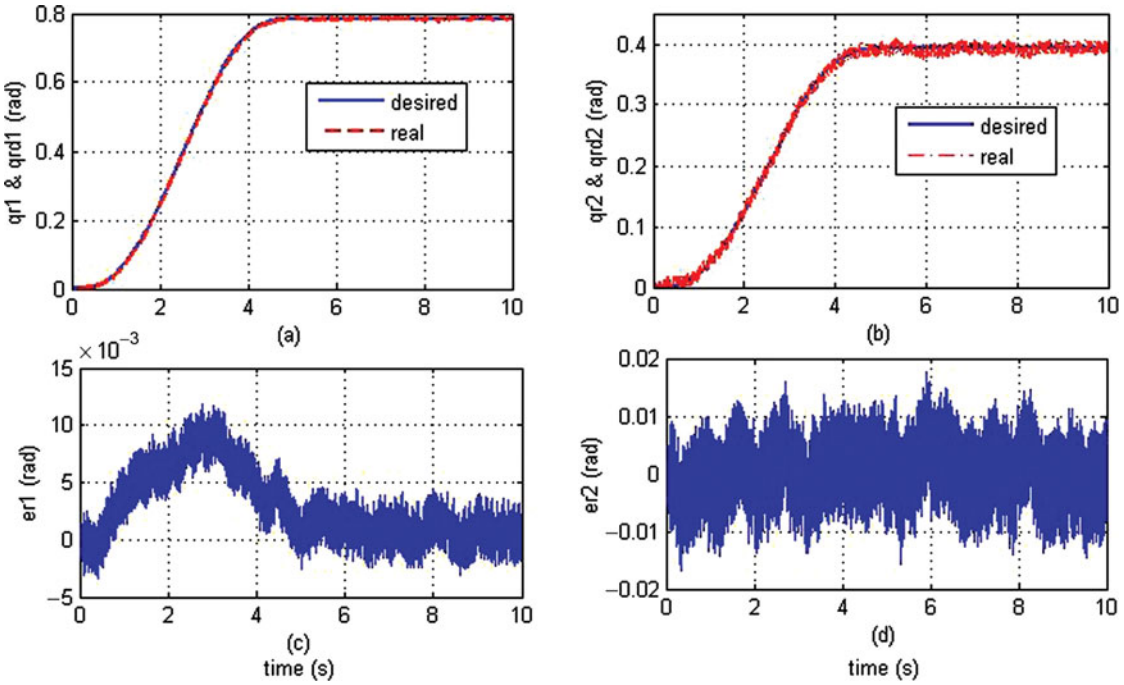


Fig. 10. PD control: (a)–(b) joint tracking trajectories, (c)–(d) joint tracking errors.

The results of the developed distributed control method were compared with a PD type control to show the contribution of this proposed control strategy using the same desired trajectories. The PD control law can be written as follows:

$$\boldsymbol{\tau} = K_p(\boldsymbol{q} - \boldsymbol{q}_d) + K_d(\dot{\boldsymbol{q}} - \dot{\boldsymbol{q}}_d), \tag{56}$$

https://doi.org/10.1017/S0263574714000459 Published online by Cambridge University Press

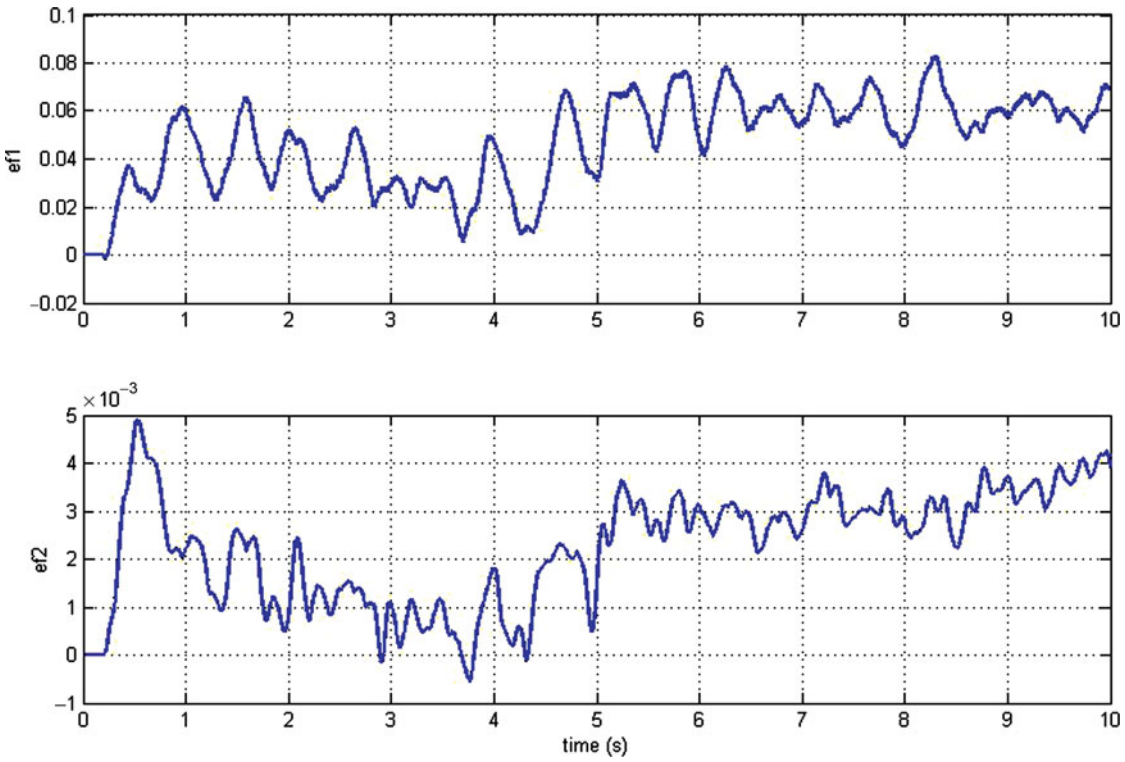


Fig. 11. PD control: errors of flexible parts.

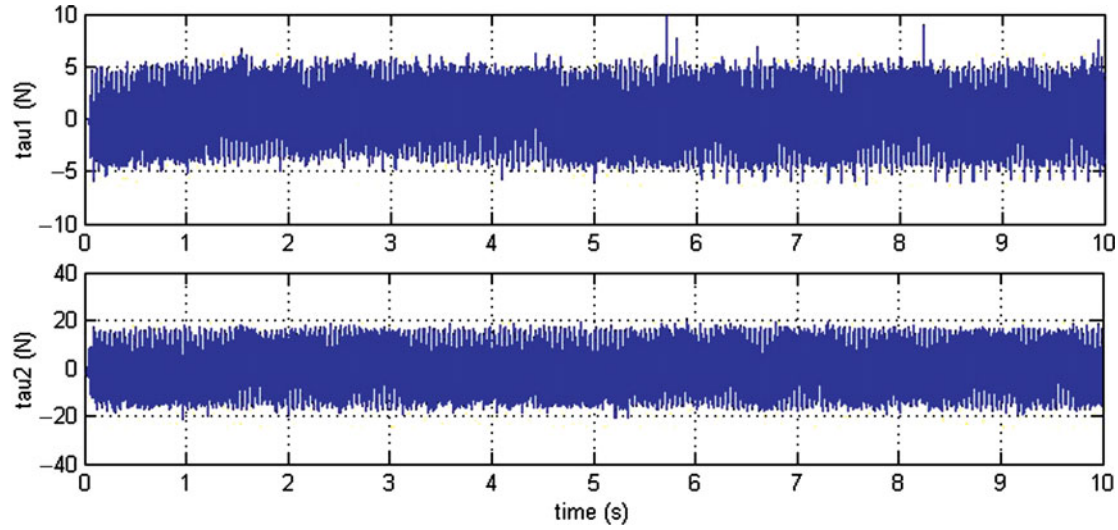


Fig. 12. PD control: input torques.

where K_p and K_d are constant gain matrices. $K_p = diag(10, 10, 10, 10)$ and $Kd = diag(8, 8, 8, 8)$. According to the experimental results, for the distributed control strategy, a good tracking in the joint space is shown in Fig. 7. This good tracking is confirmed by the very small tracking errors, less than 0.01 rad for the first joint and 0.008 rad for the second joint. For the flexible coordinates, a small error was obtained not exceeding 0.006 rad as shown in Fig. 8. The input torque is shown in Fig. 9. The errors obtained explain the ability of the distributed control strategy to cancel vibration in the links. The results of the distributed control strategy were compared with the PD controller results (Figs. 10–12). For the distributed control method, the tracking errors of the joints and the links' vibrations

https://doi.org/10.1017/S0263574714000459 Published online by Cambridge University Press

are smaller than those resulting from the PD controller. Finally, we can conclude that the distributed control strategy eliminates vibration and gives good tracking of the desired trajectories.

5. Conclusion

This paper presents a distributed control strategy for flexible-link manipulators. This strategy consists to start by controlling the last subsystem composed of the *n*th joint and link by assuming that the remaining subsystems are stable. Then, working backward one subsystem at a time toward the first subsystem, we use the same strategy. The global stability is proven using Lyapunov approach. Experimental results, compared with a PD control, show that the distributed control strategy gives good tracking and cancels the links' vibration.

References

1. R. H. Cannon, Jr. and E. Schmitz, "Initial experiments on the end-point control of a flexible one-link robot," *Int. J. Robot. Res.* **3**(3), 62–75 (1984).
2. I. Shung, "Control of a Flexible Robot Arm with Bounded Input: Optimum Step Responses," *Proceedings of the IEEE International Conference on Robotics and Automation*, Raleigh, NC, USA (Mar. 1–4, 1987) pp. 916.
3. S. C. Saini, Y. Sharma, M. Bhandari and U. Satija, "Comparison of Pole Placement and LQR Applied to Single Link Flexible Manipulator," *Proceedings of the International Conference on Communication Systems and Network Technologies (CSNT)*, Rajkot, India (May 11–13, 2012) pp. 843–847.
4. K. S. Rattan and V. Feliu, "Feedforward Control of Flexible Manipulators," *Proceedings of the IEEE International Conference on Robotics and Automation, 1992*, IEEE, Piscataway, NJ, USA (1992) pp. 788–793.
5. J. Shan, D. Sun and D. Liu, "Design for robust component synthesis vibration suppression of flexible structures with on-off actuators," *IEEE Trans Robot. Autom.* **20**(3), 512–525 (2004).
6. R. Fareh, M. R. Saad and M. Saad, "Adaptive Control for a Single Flexible Link Manipulator Using Sliding Mode Technique," Proceedings of the *6th International Multi-Conference on Systems, Signals and Devices* March 23–26, Djerba, Tunisia (2009) pp. 1–6.
7. J. H. Yang and Y. Jung Hua, "Nonlinear adaptive control for flexible-link manipulators," *IEEE Trans Robot. Autom.* **13**(1), 140 (1997).
8. S. K. Pradhan and B. Subudhi, "Real-time adaptive control of a flexible manipulator using reinforcement learning," *IEEE Trans. Autom. Science Eng.* **9**(2), 237–249 (2012).
9. A. R. Maouche and M. Attari, "CMAC Based Adaptive Control of a Flexible Link Manipulator," *Proceedings of the 35th Annual Conference of IEEE Industrial Electronics*, Porto (May 3–5, 2009) pp. 1480–1485.
10. V. G. Moudgal, "Rule-based control for a flexible-link robot," *IEEE Trans. Control Syst. Technol.* **2**(4), 392 (1994).
11. Y. Tang, "Neural network control of flexible-link manipulators using sliding mode," *Neurocomputing* **70**(1–3), 288 (2006).
12. A. Jnifene, "Experimental study on active vibration control of a single-link flexible manipulator using tools of fuzzy logic and neural networks," *IEEE Trans. Instrum. Meas.* **54**(3), 1200 (2005).
13. Y. Wang and W. Yanmin, "High-Order Nonsingular Terminal Sliding Mode Optimal Control of Two-Link Flexible Manipulators," *Proceedings of the 37th Annual Conference of the IEEE Industrial Electronics Society*, Melbourne, VIC (Nov. 7–10, 2011) pp. 3953.
14. A. Arisoy, M. Gokasan and O. S. Bogosyan, "Sliding Mode Based Position Control of a Flexible-Link Arm," *Proceedings of the 12th International Power Electronics & Motion Control Conference*, 30 Aug.–1 Sep. 2006, IEEE, Piscataway, NJ, USA (2006). pp. 402–407.
15. K. S. Fu, R. C. Gonzalez and C. S. G. Lee, *Robotics : Control, Sensing, Vision, and Intelligence* (McGraw-Hill, New York, 1987).
16. F. Khorrami, "Experimental Results on Active Control of Flexible-Link Manipulators with Embedded Piezoceramics," *Proceedings of the IEEE International Conference on Robotics and Automation*, Atlanta, GA (May 2–6, 1993) pp. 222–229.
17. D. Sun and J. K. Mills, "Control of a rotating cantilever beam using a torque actuator and a distributed piezoelectric polymer actuator," *Appl. Acoust.* **63**(8), 885 (2002).
18. K. L. Hillsley, "Vibration control of a two-link flexible robot arm," *Dyn. Control* **3**(3), 212–216 (1993).
19. R. Fareh, M. R. Saad and M. Saad, "Workspace trajectory tracking control for two-flexible-link manipulator through output redefinition," *Int. J. Model. Identif. Control* **18**(2), 119–135 (2013).
20. A. De Luca and B. Siciliano, "Closed-form dynamic model of planar multilink lightweight robots," *IEEE Trans. Syst. Man Cybern.* **21**(4), 826–839 (1991).
21. R. G. Bartle and D. R. Sherbert, *Introduction to Real Analysis* (Wiley, New York, 2000).
22. M. W. Spong and M. Vidyasagar, *Robot Dynamics and Control* (J. Wiley, New York, 1989).
23. A. De Luca and B. Siciliano, "Explicit Dynamic Modeling of a Planar Two-Link Flexible Manipulator," *Proceedings of the 29th IEEE Conference on Decision and Control Part 6*, December 5–7, Honolulu, HI, USA (1990) pp. 528–530.

https://doi.org/10.1017/S0263574714000459 Published online by Cambridge University Press

24. J. J. Craig, *Introduction to Robotics: Mechanics and Control* (Pearson/Prentice Hall, Upper Saddle River, NJ, 2005).

Appendix

Proof of proposition 1
Let us define the second term of the error dynamics (27) as follows:

$$\boldsymbol{\tau}_s = M(\boldsymbol{q})\,\ddot{\boldsymbol{u}} + C(\boldsymbol{q},\dot{\boldsymbol{q}})\,\dot{\boldsymbol{u}} + D\dot{\boldsymbol{u}} + K_d\boldsymbol{s} + K\boldsymbol{q} - L\boldsymbol{\tau}. \tag{57}$$

Using the transformation (5), the previous error dynamics is equivalent to:

$$\bar{\boldsymbol{\tau}}_s = \bar{M}(q)\,\ddot{\bar{\boldsymbol{u}}} + \bar{C}(\boldsymbol{q},\dot{\boldsymbol{q}})\,\dot{\bar{\boldsymbol{u}}} + \bar{D}\dot{\bar{\boldsymbol{u}}} + \bar{K}_d\bar{\boldsymbol{s}} + \bar{K}\bar{\boldsymbol{q}} - L\boldsymbol{\tau}, \tag{58}$$

where $\bar{M}(\boldsymbol{q}) = M(\boldsymbol{q})\,T_r$; $\bar{C}(\boldsymbol{q},\dot{\boldsymbol{q}}) = C(\boldsymbol{q},\dot{\boldsymbol{q}})\,T_r$; $\bar{D} = DT_r$; $\bar{K} = KT_r$; $\bar{L} = LT_r$; $\dot{\bar{\boldsymbol{u}}} = \dot{\boldsymbol{u}}T_r$, $\bar{\boldsymbol{s}} = \boldsymbol{s}T_r$, and $\bar{\boldsymbol{\tau}}_s = \boldsymbol{\tau}_s T_r$. For the ith subsystem τ_{si} is given as:

$$\bar{\boldsymbol{\tau}}_{\boldsymbol{si}} = \bar{M}_i^T(\boldsymbol{q})\,\ddot{\bar{\boldsymbol{u}}} + \bar{C}_i^T(\boldsymbol{q},\dot{\boldsymbol{q}})\,\dot{\bar{\boldsymbol{u}}} + \bar{D}_i^T\dot{\bar{\boldsymbol{u}}} + \bar{K}_i^T\bar{\boldsymbol{q}} + \bar{K}_{di}^T\bar{\boldsymbol{s}} - \bar{L}_i\tau_i, \tag{59}$$

where $\bar{M}_i^T(\boldsymbol{q}) = \begin{bmatrix}\bar{M}_{i1} & \cdots & \bar{M}_{in}\end{bmatrix}^T$; $\bar{C}_i^T(\boldsymbol{q},\dot{\boldsymbol{q}}) = \begin{bmatrix}\bar{C}_{i1} & \cdots & \bar{C}_{in}\end{bmatrix}^T$; $\bar{K}_i^T = \begin{bmatrix}\bar{K}_{i1} & \cdots & \bar{K}_{in}\end{bmatrix}^T$; $\bar{D}_i^T = \begin{bmatrix}\bar{D}_{i1} & \cdots & \bar{D}_{in}\end{bmatrix}^T$; $\bar{K}_{di}^T = \begin{bmatrix}\bar{K}_{di1} & \cdots & \bar{K}_{din}\end{bmatrix}^T$ and $\bar{L}_i = \begin{bmatrix}0\ldots010\cdots0\\ 0\ldots000\cdots0\end{bmatrix}_{2\times n}$.

Using Taylor series, we can write:

$$\bar{M}_{ij}(\boldsymbol{q}) = \bar{M}_{ij}(\bar{\boldsymbol{q}}) = \bar{M}_{ij}(\bar{\mathbb{q}}_i) + D\bar{M}_{ij}(\bar{\mathbb{q}}_i)^T(\bar{\boldsymbol{q}} - \bar{\mathbb{q}}_i) + \frac{1}{2!}(\bar{\boldsymbol{q}} - \bar{\mathbb{q}}_i)^T\left\{D^2\bar{M}_{ij}(\bar{\mathbb{q}}_i)\right\}(\bar{\boldsymbol{q}} - \bar{\mathbb{q}}_i) + \ldots$$

where $D\bar{M}_{ij}(\bar{\mathbb{q}}_i)$ is the gradient of $\bar{M}_{ij}$ evaluated at $\bar{\boldsymbol{q}} = \bar{\mathbb{q}}_{\boldsymbol{i}}$ and $D^2\bar{M}_{ij}(\bar{\mathbb{q}}_{\boldsymbol{i}})$ is a Hessian matrix. Then, we can write:

$$\bar{M}_{ij}(q) = \bar{M}_{ij}(\bar{\mathbb{q}}_i) + \left.\frac{\partial\bar{M}_{ij}(\boldsymbol{q})}{\partial\left[\boldsymbol{q_1}\ \cdots\ \boldsymbol{q_{i-1}}\boldsymbol{q_{i+1}}\cdots\boldsymbol{q_n}\right]}\right|_{\begin{bmatrix}\boldsymbol{q_{1d}}\\ \vdots\\ \boldsymbol{q_{(i-1)d}}\\ \boldsymbol{q(i+1)d}\\ \vdots\\ \boldsymbol{q_{nd}}\end{bmatrix}}\begin{bmatrix}\boldsymbol{q_1} - \boldsymbol{q_{1d}}\\ \vdots\\ \boldsymbol{q_{i-1}} - \boldsymbol{q_{(i-1)d}}\\ \boldsymbol{q_{i+1}} - \boldsymbol{q_{(i+1)d}}\\ \vdots\\ \boldsymbol{q_{n-q_{nd}}}\end{bmatrix} + R_{M_{ij}}(\tilde{\boldsymbol{q}}_j)$$

$$= \bar{M}_{ij}(\bar{\mathbb{q}}_i) - \sum_{\substack{j=1\\ j\neq i}}^{n}\left.\frac{\partial\bar{M}_{ij}(q)}{\partial q_j}\right|_{q_{jd}}\tilde{\boldsymbol{q}}_j + R_{M_{ij}}(\tilde{\boldsymbol{q}}_j)$$

$$= \bar{M}_{ij}(\bar{\mathbb{q}}_i) - \delta\bar{M}_{ij},$$

where

$$\delta\bar{M}_{ij} = \sum_{\substack{j=1\\ j\neq i}}^{n}\left.\frac{\partial\bar{M}_{ij}(\boldsymbol{q})}{\partial\boldsymbol{q_j}}\right|_{\boldsymbol{q_{jd}}}\tilde{\boldsymbol{q}}_{\boldsymbol{j}} - R_{M_{ij}}(\tilde{\boldsymbol{q}}_{\boldsymbol{j}})\,and\,R_{M_{ij}}$$

https://doi.org/10.1017/S0263574714000459 Published online by Cambridge University Press

is the remaining terms given as follows:

$$R_{M_{ij}}\left(\tilde{\boldsymbol{q}}_j\right) = \bar{M}_{ij}\left(\boldsymbol{q}\right) - \bar{M}_{ij}\left(\bar{\mathbb{q}}_i\right) + \sum_{\substack{j=1 \\ j\neq i}}^{n} \left.\frac{\partial \bar{M}_{ij}\left(\boldsymbol{q}\right)}{\partial \boldsymbol{q}_j}\right|_{\boldsymbol{q}_{jd}} \tilde{\boldsymbol{q}}_j.$$

Using the same strategy of Taylor series for M_{ii} we can write:

$$\bar{M}_{ii}\left(\boldsymbol{q}\right) = \bar{M}_{ii}\left(\bar{\boldsymbol{q}}\right) = \bar{M}_{ii}\left(\bar{\mathbb{q}}_i\right) - \sum_{\substack{j=1 \\ j\neq i}}^{n} \left.\frac{\partial \bar{M}_{ii}\left(\boldsymbol{q}\right)}{\partial \boldsymbol{q}_j}\right|_{\boldsymbol{q}_{jd}} \tilde{\boldsymbol{q}}_j + R_{M_{ii}}\left(\tilde{\boldsymbol{q}}_j\right) = \bar{M}_{ii}\left(\bar{\mathbb{q}}_i\right) - \delta\bar{M}_{ii},$$

where

$$\delta\bar{M}_{ii} = \sum_{\substack{j=1 \\ j\neq i}}^{n} \left.\frac{\partial \bar{M}_{ii}(\boldsymbol{q})}{\partial \boldsymbol{q}_j}\right|_{\boldsymbol{q}_{jd}} \tilde{\boldsymbol{q}}_j + R_{M_{ii}}(\tilde{\boldsymbol{q}}_j).$$

$R_{M_{ii}}$ and $R_{M_{ii}}$ are the high-order terms of the Taylor series for $\bar{M}_{ii}(\boldsymbol{q})$. Then, we can write:

$$\begin{aligned} \bar{M}_i^T(\boldsymbol{q}) &= \bar{M}_i^T(\bar{\boldsymbol{q}}) = \bar{M}_i^T(\bar{\mathbb{q}}_i) - \delta\bar{M}_i^T, \\ \bar{C}_i^T(\boldsymbol{q}, \dot{\boldsymbol{q}}) &= \bar{C}_i^T(\bar{\boldsymbol{q}}, \dot{\bar{\boldsymbol{q}}}) = \bar{C}_i^T(\bar{\mathbb{q}}_i, \dot{\bar{\mathbb{q}}}_i) - \delta\bar{C}_i^T, \end{aligned} \tag{60}$$

and

$$\bar{\boldsymbol{\tau}}_{\boldsymbol{si}} = \bar{M}_i^T\left(\bar{\mathbb{q}}_{\boldsymbol{i}}\right)\ddot{\bar{\boldsymbol{u}}} + \bar{C}_i^T\left(\bar{\mathbb{q}}_{\boldsymbol{i}}, \dot{\bar{\mathbb{q}}}_i\right)\dot{\bar{\boldsymbol{u}}} - \delta\bar{M}_i^T\ddot{\bar{\boldsymbol{u}}} - \delta\bar{C}_i^T\dot{\bar{\boldsymbol{u}}} + \bar{D}_i^T\dot{\bar{\boldsymbol{u}}} + \bar{K}_i^T\bar{\boldsymbol{q}} + \bar{K}_{di}^T\bar{\boldsymbol{s}} - \bar{L}_i\tau_i. \tag{61}$$

Using (19) and (20), Eq. (61) can be written as follows:

$$\bar{\boldsymbol{\tau}}_{si} = \begin{bmatrix} v_{ri}\left(\bar{\mathbb{q}}_i\right) - \delta\tau_{ri} - \tau_i \\ v_{fi}\left(\bar{\mathbb{q}}_i\right) + \delta\tau_{fi} \end{bmatrix}. \tag{62}$$

Using (18), we can deduce:

$$\bar{\boldsymbol{\tau}}_{\boldsymbol{si}} = \begin{bmatrix} -T_i \\ v_{fi}\left(\bar{\mathbb{q}}_i\right) + \delta\tau_{fi} \end{bmatrix}. \tag{63}$$

Then,

$$M\left(\boldsymbol{q}\right)\dot{\boldsymbol{s}} + C\left(\boldsymbol{q}, \dot{\boldsymbol{q}}\right)\boldsymbol{s} + D\boldsymbol{s} + K_d\boldsymbol{s} = \begin{bmatrix} -\boldsymbol{T} \\ \boldsymbol{v}_f + \boldsymbol{\delta\tau}_f \end{bmatrix}. \tag{64}$$

https://doi.org/10.1017/S0263574714000459 Published online by Cambridge University Press